

A Holocene moraine chronology at Mount Rainier, Washington
based on tephrochronology and surface-exposure ages

Peter F. Apostle

A thesis submitted in partial fulfillment
of the requirements for the degree of

Master of Science

University of Washington

2004

Program Authorized to Offer Degree:
Department of Geological Sciences

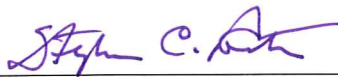
University of Washington
Graduate School

This is to certify that I have examined this copy of a master's thesis by

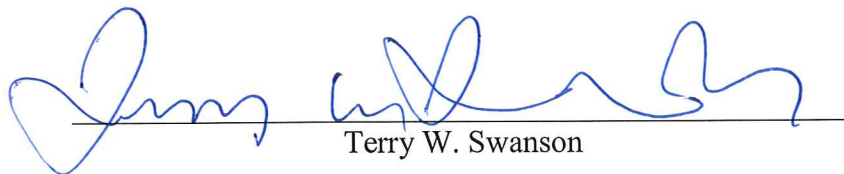
Peter F. Apostle

and have found that it is complete and satisfactory in all aspects,
and that any and all revisions required by the final
examining committee have been made.

Committee Members:



Stephen C. Porter



Terry W. Swanson

Date: MARCH 9, 2004

In presenting this thesis in partial fulfillment of the requirements for a master's degree at the University of Washington, I agree that the Library shall make its copies freely available for inspection. I further agree that extensive copying of this thesis is allowable only for scholarly purposes, consistent with "fair use" as prescribed in the U.S. Copyright Law. Any other reproduction for any purposes or by any means shall not be allowed without my written permission.

Signature



Date

MARCH 9, 2004

University of Washington

Abstract

A Holocene moraine chronology at Mount Rainier, Washington
based on tephrochronology and surface-exposure ages

Peter F. Apostle

Chair of the Supervisory Committee:
Professor Stephen C. Porter
Department of Geological Sciences

Previous reconnaissance mapping of latest Pleistocene and Holocene drift on Mount Rainier, Washington has been refined locally, the limits of each drift being more accurately determined. The age assignments of the mapped moraines are based on tephrochronology which provides a reliable, but imprecise basis for dating individual moraines. Rock samples were also collected from boulders and bedrock surfaces associated with the outer moraines at each of four sites for obtaining ^{36}Cl surface-exposure dates. A latest-Pleistocene or early Holocene glacier advance was followed by a middle-Neoglacial advance that deposited Burroughs Mountain drift, and by two late Neoglacial advances, marked by Older and Younger Garda drift. However, the outermost moraine at each locality records a McNeely or an early Holocene advance, but cannot be more-closely dated. Some of the resulting ^{36}Cl surface-exposure ages are anomalous, likely as a result of a thick snowcover that shielded the sites. The resulting data were used to assess this effect on the surface-exposure ages. A thick snowcover during mid- to late-Holocene time at the moraine sites likely reduced surface-exposure ages by ca. 50% of their expected values.

TABLE OF CONTENTS

	PAGE
LIST OF FIGURES.....	iii
LIST OF TABLES.....	iv
1. INTRODUCTION.....	1
1.1 HOLOCENE PALEOCLIMATE AND GLACIER VARIATIONS.....	1
1.2 LATEST PLEISTOCENE AND HOLOCENE GLACIER VARIATIONS IN NORTH AMERICA.....	2
1.3 LATEST PLEISTOCENE AND HOLOCENE GLACIER VARIATIONS ON MOUNT RAINIER.....	4
1.4 FOSSIL POLLEN RECORDS OF LATEST PLEISTOCENE AND HOLOCENE CLIMATE IN WASHINGTON STATE.....	8
1.5 PROJECT SCOPE.....	9
2. CHRONOLOGICAL METHODS.....	10
2.1 TEPHROCHRONOLOGY.....	10
2.1.1 TEPHRA SEQUENCE AND AGES IN THE CASCADES.....	11
2.1.2 IDENTIFICATION AND DATING OF TEPHRA LAYERS.....	11
2.2 SURFACE-EXPOSURE DATING.....	14
2.2.1 FACTORS INFLUENCING EXPOSURE AGES.....	14
2.2.2 SAMPLE COLLECTION.....	17
2.2.3 LABORATORY METHODS.....	17
2.3 EFFECT ON SURFACE-EXPOSURE AGES OF SEASONAL AND PERENNIAL SNOWPACKS.....	24
3. HOLOCENE GLACIAL RECORD ON MOUNT RAINIER.....	34
3.1 FIELD AREA.....	34
3.2 PARADISE GLACIER SITE.....	34
3.3 WILLIWAKAS GLACIER/FAIRY FALLS SITE.....	41
3.4 BERKELEY PARK SITE.....	50
3.5 GRANITE CREEK SITE.....	59
3.6 TALUS AND COLLUVIAL FAN STRATIGRAPHY AND CHRONOLOGY.....	63

4. SYNTHESIS	67
4.1 EFFECTS OF CLIMATE ON MASS BALANCE ON MOUNT RAINIER.....	67
4.2 LATE PLEISTOCENE AND HOLOCENE EQUILIBRIUM LINE ALTITUDES.....	68
4.2.1 PARADISE GLACIER EQUILIBRIUM LINE ALTITUDES.....	69
4.2.2 WILLIWAKAS GLACIER EQUILIBRIUM LINE ALTITUDES.....	70
4.2.3 BERKELEY PARK GLACIER EQUILIBRIUM LINE ALTITUDES.....	70
4.2.4 GRANITE CREEK GLACIER EQUILIBRIUM LINE ALTITUDES.....	71
4.3 COMPARISON WITH PREVIOUS RESEARCH.....	72
4.4 CONCLUSION.....	73
 REFERENCES.....	 75

**POCKET MATERIAL: PLATE 1: HOLOCENE MORaine CHRONOLOGY OF
MOUNT RAINIER, WASHINGTON (MAP)**

LIST OF FIGURES

	PAGE
FIGURE 1: Idealized chronostratigraphic section of major surficial Deposits on Mount Rainier.....	5
FIGURE 2: Little Ice Age moraine ages on Mount Rainier.....	6
FIGURE 3: Idealized chronostratigraphic section of major tephra units on Mount Rainier used in this study.....	7
FIGURE 4: Boulder exhumation explanation.....	16
FIGURE 5: Map of Paradise Lahar calibration site.....	25
FIGURE 6: Graph of Paradise Lahar surface-exposure ages.....	33
FIGURE 7: Map of the Paradise Glacier field site.....	35
FIGURE 8: Profile of Paradise Glacier moraines with surface-exposure age sample locations.....	36
FIGURE 9: Graph of Paradise Glacier surface-exposure ages.....	39
FIGURE 10: Profile of the glacier that deposited the Paradise Glacier moraines.....	42
FIGURE 11: Paradise Glacier and Williwakas Glacier surface altitude contour map.....	44
FIGURE 12: Map of the Williwakas Glacier/Fairy Falls field site.....	45
FIGURE 13: Graph of Williwakas Glacier/Fairy Falls surface-exposure ages.....	47
FIGURE 14: Profile of Williwakas Glacier/Fairy Falls moraines with surface-exposure age sample locations.....	48
FIGURE 15: Profile of the glacier that deposited the Williwakas Glacier/Fairy Falls moraines.....	51
FIGURE 16: Map of the Berkeley Park and Granite Creek field sites.....	52
FIGURE 17: Profile of Berkeley Park moraine with surface-exposure age sample locations.....	53
FIGURE 18: Graph of Berkeley Park surface-exposure ages.....	55
FIGURE 19: Profile of the glacier that deposited the Berkeley Park moraine.....	57
FIGURE 20: Granite Creek and Berkeley Park glacier surface altitude contour map.....	58
FIGURE 21: Profile of Granite Creek moraines with surface-exposure age sample locations.....	60
FIGURE 22: Graph of Granite Creek surface-exposure ages.....	62
FIGURE 23: Profile of the glacier that deposited the Granite Creek moraines.....	64
FIGURE 24: Idealized chronostratigraphic section of talus near Paradise.....	66

LIST OF TABLES

	PAGE
TABLE 1: Tephra layer chemical composition data.....	13
TABLES 2a-e: Surface-exposure age sample data	
TABLE 2a: Field data.....	19
TABLE 2b: Shielding data.....	20
TABLE 2c: Total chlorine data.....	21
TABLE 2d: Elemental oxide composition data.....	22
TABLE 2e: Elemental concentration data.....	23
TABLE 3: Historical Mount Rainier snowpack data.....	26
TABLE 4: Radiocarbon dates of the Paradise Lahar.....	27
TABLE 5: Snowpack values for exposure age calculation.....	29
TABLE 6: Surface-exposure ages for the Paradise Lahar.....	32
TABLE 7: Surface-exposure ages for the Paradise Glacier field site.....	38
TABLE 8: Surface-exposure ages for the Fairy Falls field site.....	46
TABLE 9: Surface-exposure ages for the Berkeley Park field site.....	54
TABLE 10: Surface-exposure ages for the Granite Creek field site.....	61

ACKNOWLEDGEMENTS

I want to express my great appreciation of the direction Stephen Porter has given me throughout this research. His advise began with the suggestion of this research project in the summer of 1997, before I had even applied for graduate admission to the University of Washington. Steve always made time for me a top priority in his incredibly crowded schedule. Having the access to his encyclopedic knowledge of geology and the privilege to study under him has been one of the great honors of my life.

I am indebted to Terry Swanson who also provided guidance throughout this research project. In addition, Terry provided his laboratory and funding for processing and dating rock samples. Terry's enthusiasm and advice also saw me through the many pitfalls of being a graduate student.

John Stone has taught me the theoretical background and laboratory techniques for working with cosmogenic isotopes. John has also provided informal advice throughout this research. All ^{36}Cl measurements were performed with the help of Mark Caffee at Lawrence Livermore National Laboratory in Livermore, California. Dan McCrumb helped with all techniques used in Terry Swanson's laboratory.

Chris Newhall, Tom Sisson, and Pat Pringle all provided advice and information on the volcanic deposits found on Mount Rainier. Carolyn Driedger supplied aerial photographs and information on the current state of Mount Rainier's glaciers. Barbara Samora provided access to aerial photographs at Mount Rainier National Park headquarters and permission for the fieldwork in the park. Darin Swinney supplied Mount Rainier National Park GIS data.

I cannot fail to mention the help in the field from friends and fellow graduate students Steve Thompson, Greg Balco, and Jeff Witter. Nate Chutas, another fellow graduate student, has provided friendship, advice, encouragement, and his lonely belief in my will and ability to complete this thesis will always be appreciated.

Finally, I would like to thank my parents and sister for their support and patience through all of my adventures and crazy ideas, including this one.

DEDICATION

Sean Ryan was a friend and fellow geology student at the University of California, Santa Cruz. Sean's geologic studies of the Barbados subduction zone combined his interest in tectonics and an interest in marine geology, inherited from his father, Dr. William Ryan. Sean died from a fall during a nighttime rescue attempt high on Mount Rainier while working as a junior climbing ranger during the summer of 1995. This thesis is dedicated to him.

1. INTRODUCTION

1.1 HOLOCENE PALEOCLIMATE AND GLACIER VARIATIONS

If we are to place modern climatic shifts, anthropogenic and natural, into perspective, climate-proxy records are needed to tell us how fast, where, and when previous climatic shifts occurred. Climate-proxy records ranging from millennial to decadal time scales are necessary, as previous research shows that important shifts in climate occur on these short time scales. Recently discovered Holocene climate proxies have affirmed that cool/warm and wet/dry oscillations occurred throughout the Holocene (Alley et al., 1997). For example, a ca. 400-year-long cold period, centered on 8200 calibrated ^{14}C years before the present (cal yr BP)¹, appears in the paleotemperature signal of Greenland ice-core records (Alley et al., 1997). The wide geographic extent of this climate anomaly has been confirmed by coeval climatic events in different regions of the world [e.g., cold conditions in northern Sweden (Karlén and Denton, 1976) and southern Germany (von Grafenstein et al., 1998); fresh, cool surface-water conditions in the North Atlantic (Lehman and Keigwin, 1992); and windy conditions in the Cariaco Basin in the southern Caribbean Sea (Hughen et al., 1996)]. This brief event has been attributed to reduced sea-surface salinity and altered circulation of the North Atlantic Ocean. The disruption of North Atlantic circulation may have been caused by an abrupt discharge of freshwater from glacial lakes impounded beyond the retreating Laurentide ice sheet in North America (Barber et al., 1999).

Climatic shifts also have occurred in the middle to late Holocene over much of the world including western North America, during an interval termed Neoglaciation (Porter and Denton, 1967). Detailed Neoglacial chronologies are best developed in Europe and North America (Porter, 2000). Continuous high-resolution records of Neoglacial climatic shifts appear in Greenland ice cores and also are recorded in North Atlantic deep-sea sediments (Andrews and Giraudeau, 2003).

¹ Whenever possible ages reported in this study are presented as calendar years before the present (cal yr B.P.). Present is defined as 1950 A.D. for all ages converted from radiocarbon ages. ^{36}Cl surface-exposure ages will be discussed in Section 2.3.

1.2 LATEST PLEISTOCENE AND HOLOCENE GLACIER VARIATIONS IN NORTH AMERICA

Evidence of late-glacial, early Holocene, and Neoglacial ice advances has been reported from the American and Canadian rocky mountains (Davis, 1988; Luckman, 2000; Osborn and Luckman, 1988), the Cascade Range (Begét, 1981; Burbank, 1981; Heine, 1997; Thomas et al., 2000; Waitt et al., 1982), the Sierra Nevada (Clark and Gillespie, 1997), the Canadian Coast Ranges (Calkin et al., 2001; Clague and Matthews, 1996; Evans, 1997; Porter and Denton, 1967; Smith and Desloges, 2000), and Alaska (Calkin and Ellis, 1982; Calkin et al., 2001). While the evidence for late-glacial ice advances is widespread, the chronology generally is poorly established, for it is based mostly on minimum limiting ^{14}C dates (Davis, 1988; Heine, 1997). Chronologies of possible early Holocene ice advance are less-well constrained, with evidence only reported in the northern Cascade Range of Washington (Begét, 1981; Reasoner et al., 2001; Thomas et al., 2000; Waitt et al., 1982). By contrast, evidence of middle and late Neoglacial advances has been reported widely in the western U.S. and Canada (e.g., Burbank, 1981; Calkin et al., 2001; Davis, 1988; Denton and Karlén, 1973; Driedger, 1986; Driedger and Kennard, 1984; Osborn and Luckman, 1988; Porter, 1981a; Sigafos and Hendricks, 1961 and 1972).

Late-glacial advances (i.e., ca. 13,000-10,000 ^{14}C yr BP) in western North America were more extensive than Holocene advances (Crandell, 1969; Davis, 1988). In the U.S., an advance just prior to 13,000 cal yr BP (11,000 ^{14}C yr BP) has been reported for mountains in Colorado, Montana, California, and Washington (Davis, 1988; Heine, 1997). Evidence of one or two advances has been found in the Sierra Nevada (Clark and Gillespie, 1997). At Mount Rainier, the timing and extent of late-glacial ice advances apparently does not match that of Younger Dryas-age ice advances in Europe (Heine, 1998). There is field evidence of an advance, inferred to fall between 11,000 and 10,000 cal yr BP (10,000-9000 ^{14}C yr BP), in most western states except Idaho, Oregon,

Nevada, Arizona, and New Mexico, (Davis, 1988), but the chronology relies mainly on minimum ages, and therefore is provisional.

Little credible evidence of a reported pre-Neoglacial, early Holocene cooling event at ca. 8200 cal yr BP exists in western North America. Inferred early Holocene glacier advances at Glacier Peak, Washington (Begét, 1981) and Mount Baker, Washington (Thomas et al., 2000) have been questioned (Davis, 1988; Reasoner et al., 2001). No ice advances have been recognized in western North America between 8000 and 5600 cal yr BP (Miller, 1969; Porter and Denton, 1967), a period falling within the hypsithermal interval.

North American evidence suggests that glaciers fluctuated broadly in phase during Neoglaciation. The timing of intervals of expansion and contraction vary regionally by a few hundred years. The early Neoglacial period began in North America ca. 5600-5300 cal yr BP for ice advances in the northern Cascade Range (Miller, 1969; Porter and Denton, 1967), and ca. 5000 cal yr BP for glacier advances in southern South America (Porter, 2000). Evidence for the timing of a mid-Neoglacial advance, between ca. 4000 and 2700 cal yr BP (~ 4700 ^{14}C yr BP), comes from Alaska and northwestern Canada (Calkin and Ellis, 1982; Calkin et al., 2001; Denton and Karlén, 1973), and across the western US (Davis, 1988). Deposits of pre-Little Ice Age (late-Neoglacial) ice advances are sporadic and generally poorly dated across western North America (Davis, 1988).

The term Little Ice Age (LIA) was introduced by Mathes (1939), and refers to the interval of glacial expansion from ca. 1250-1850 A. D. (Porter, 1986). It is characterized by three main phases, the first beginning ca. 1250 A. D., the second culminating ca. 1600-1650 A. D., and the third culminating ca. 1810-1825 (or ca. 1850) A.D. LIA advances are well documented across most of western North America (Porter and Denton, 1967; Burbank, 1981; Davis, 1988; Miller, 1964; Osborn and Luckman, 1988; Bradley and Jones, 1995). However, the best-documented LIA chronologies have been developed in the European

Alps. In the Alps the chronologies rely on instrumental records (back to 1760 A. D.) and first-person historical records that cover much of the middle and late LIA (Orombelli and Porter, 1982; Zumbühl, 1980). LIA advances are similar in relative extent and timing across the western U.S. (Calkin et al., 2001; Davis, 1988; Denton and Karlén, 1973; Luckman, 2000). The widespread LIA evidence is the result of its young age and good preservation of the deposits.

1.3 LATEST PLEISTOCENE AND HOLOCENE GLACIER VARIATIONS ON MOUNT RAINIER

Previous work on and around Mount Rainier has disclosed field evidence of two or three late-glacial and Holocene glacier advances (Crandell, 1969; Heine, 1997, 1998) (Fig. 1). The oldest late-glacial advance on the mountain (>13,200 cal yr BP) was designated McNeely 1 by Heine (1997). According to limited age control, the McNeely 1 advance was not correlative with Younger Dryas advances elsewhere in the world (Heine, 1997). The age control relies on three bulk lake-sediment samples taken from varying depths inside McNeely 1 moraines to provide minimum limiting radiocarbon dates for the advance. This ice advance may correlate with the Recess Peak advance in the Sierra Nevada of California, ca. 13,100 cal yr BP (Clark and Gillespie, 1997). According to Heine (1997), the McNeely 2 advance lasted from ca. 10,900 to 9950 cal yr BP.

Neoglacial ice advances on Mount Rainier previously were dated using widespread tephra layers that are bracketed by radiocarbon ages (Crandell and Miller, 1964) (Figs. 1, 2, 3). The radiocarbon chronology was confirmed by Mullineaux (1974). Crandell and Miller (1964) attributed deposits of the Burroughs Mountain Drift to a mid-Neoglacial advance between ca. 4000 and 2200 cal yr BP, based on the stratigraphic position of drift above tephra layer Yn (3400 ^{14}C yr BP) and below tephra layer C (2200 ^{14}C yr BP) (Figs. 1). Crandell and Miller (1964) named late Neoglacial deposits on Mount Rainier the Garda drift, divisible into Older and Younger Garda drift. The older drift has limiting

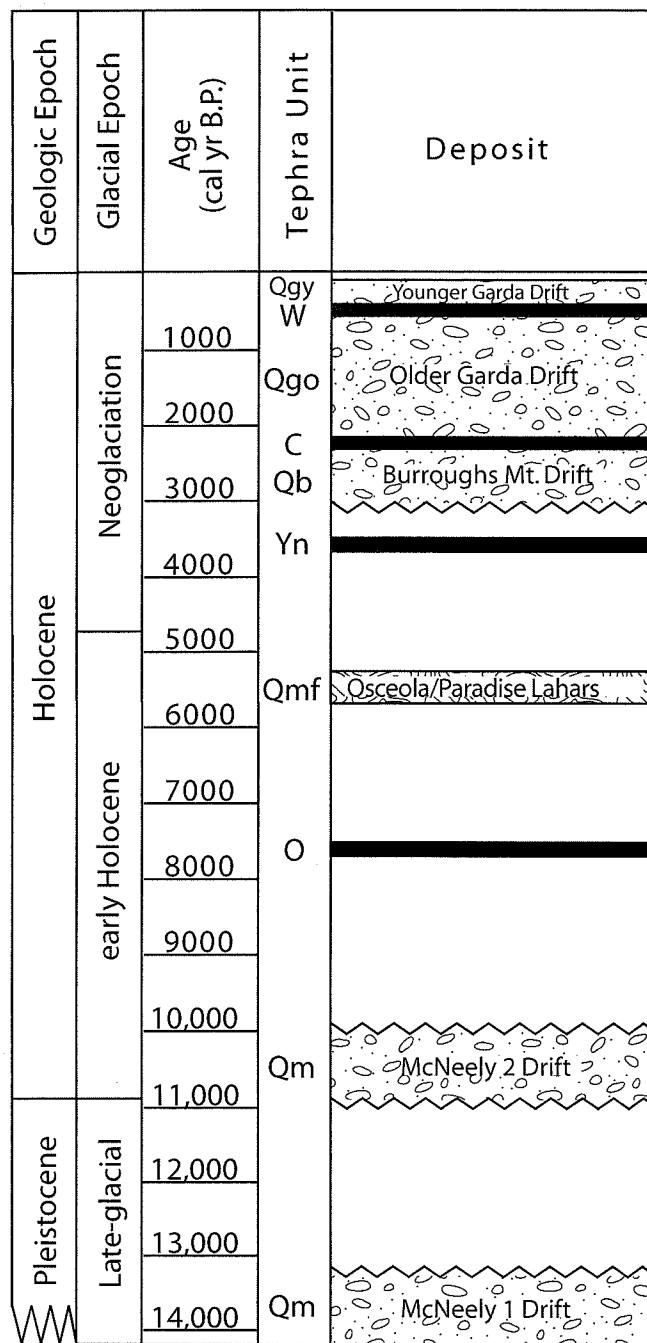


Figure 1: Idealized chronostratigraphic section of major surficial deposits on Mount Rainier. The section shows late-glacial and Holocene glacial deposits, major tephra units, and Osceola and Paradise lahars discussed by Crandell (1969) and Heine (1997) at Mount Rainier.







Mean Unit Age (cal yr BP)	Source Volcano	Thickness (cm)	Grain Size (mm)	Unit	Graphic Section	Description
470	Rainier	0-8	<1.0	W		White, sand-sized ash, at or near surface
1000						Colluvium
2225	Rainier	0-30	15	C		Brownish lapilli deposit at or near surface
3000						Colluvium
3650	St. Helens	2-30	1.0	Yn		Yellowish, coarse ash with sparse black lithic particles
5000						Thin Rainier tephra units mostly interbedded with brownish fine to coarse sandy colluvium
7000	Mazama	2-7	<0.4	O		Reddish-yellow to light pale-yellow- colored ash, widespread and well preserved
7650						Sandy Colluvium
9000	Rainier	0-15	40	R		Reddish-brown lapilli below layer O, not found south of summit
10,025						Rainier andesite, pinkish-red to grayish, Quaternary in age
>10,000	Rainier			Qra		

Figure 3: Idealized chronostratigraphic section of major tephra units on Mount Rainier used in this study. Tephra layers are used to assign relative ages to glacial deposits (Mullineaux, 1974). Grain size is the average size 7 km from the summit along the primary axis of the tephra lobe.

ages of 2200-1480 A.D. based on its stratigraphic position between tephra layers C and W (1480 A.D.). Younger Garda Drift, with a tephrochronologic age of <1480 A.D., is correlative with late LIA advances studied by Burbank (1981); Crandell and Miller (1964); Driedger (1986); Driedger and Kennard (1984); Porter (1981a); and Sigafos and Hendricks (1961, 1972). Nine of the largest glaciers on Mount Rainier have produced Younger Garda moraines that have been extensively studied and dated using lichenometry and dendrochronology (Burbank 1981; Crandell and Miller 1964; Driedger 1986; Porter 1981a; Sigafos and Hendricks 1961 and 1972). These studies have resulted in a refined late Neoglacial history of nine glaciers (Fig. 2).

1.4 FOSSIL POLLEN RECORDS OF LATEST PLEISTOCENE AND HOLOCENE CLIMATE IN WASHINGTON STATE

Pollen data from the southern Puget Lowland of Washington support Crandell's (1969) and Heine's (1997) regional climate chronology by showing evidence of a warming climate by 12,500 cal yr BP on the western side of the Cascade Range (Barnosky, 1983). The pollen record indicates that the warmest, driest part of the Holocene occurred between 10,000 and 7000 cal yr BP, i.e., the early hypsithermal interval. This warm, dry period ended by 6000 cal yr BP when cooler, more-humid conditions returned, leading to Neoglacial ice advances. Pollen records spanning 6000-0 cal yr BP from ponds on Mount Rainier near two of the field sites in this project are consistent with the glacial history proposed by Crandell (1969). They show that Neoglacial cooling may not have begun on Mount Rainier until as late as 3700 cal yr BP (Dunwiddie, 1986). However, the lack of older radiocarbon-dated sediment in the ponds makes this conclusion questionable.

1.5 PROJECT SCOPE

This study examines high-altitude moraines on Mount Rainier, a 4393-m-high volcano in the central Cascade Range of Washington state (Plate 1), to improve the Holocene glacial chronology on the mountain. Mount Rainier provides exceptional sites to study records of Holocene climatic change. As a popular national park near large urban centers, access to field sites is expeditious and easy. Due to its height, latitude, and high annual precipitation, Mount Rainier has more glaciers on its flanks than any other mountain in the contiguous United States.

Climate change can lead to changes in glacier mass balance, inferences about which can be obtained from glacial deposits and landforms. Holocene paleoclimate data exist on Mount Rainier in the form of interbedded glacial, periglacial, and volcanic deposits (Fig. 1). Most of the Holocene volcanic deposits on Mount Rainier are the result of small eruptions that would not have a prolonged (ca. 10^2 yr) affect on climate. These eruptions apparently were not responsible for any climate change that generated Holocene glacial deposits on Mount Rainier. They include tephra layer O, the product of the largest Holocene eruption in the Pacific Northwest. However, if such eruptions were part of a worldwide episode of increased volcanic activity, global temperatures may have dropped, forcing snowlines lower and possibly producing brief glacier advances (Porter, 1981b).

Crandell's (1969) mapping was refined in this study at four sites on Mount Rainier (Plate 1). An additional goal of this project was to test the use of surface-exposure dating to obtain ages for the glacial deposits. A better understanding of the Holocene climate on Mount Rainier and its relation to the larger-scale climate of the western U.S. and Canada were the ultimate goals of this project.

2. CHRONOLOGICAL METHODS USED IN THIS STUDY

Dendrochronologic methods were not used in this study because the moraines lie at or above the local tree-line, and support no or few trees. Dendrochronology uses the number yearly rings of the oldest tree on a moraine to determine a minimum age for the moraine. Sigafos and Hendricks (1961, 1972) used dendrochronology to date the maximum LIA moraine of Nisqually Glacier (Fig. 2) to 1840 A. D. They also determined that conifer ecesis, the time after deposition of a moraine until trees begin growing, is five years for trees in the forested valleys of Mount Rainier (Sigafos and Hendricks, 1969). McCarthy and Luckman (1993) determined conifer ecesis to be 5-60 yr in the Canadian Cordillera.

The general lack of preserved organic matter in or around the studied moraines limited the use of radiocarbon dating for developing a chronology. The trees, shrubs, and lichens at the altitude of the moraines decompose rapidly after they die. The widespread distribution of perennial snowpatches near the field areas in this study decreases the reliability of assigning lichenometric ages to moraines, as moraine boulders hosting lichen may have been periodically covered by perennial snow since their deposition (Frederick, 1980).

2.1 TEPHROCHRONOLOGY

Holocene eruptions of Mount Rainier and neighboring Cascade volcanoes have produced numerous and well-preserved tephra layers that can be used to assign limiting and relative ages to the glacial deposits (Fig. 3). Tephra units are used to assign relative ages to glacial and periglacial sediments using their stratigraphic position relative to the tephra layers (Mullineaux, 1974).

2.1.1 TEPHRA SEQUENCE AND AGES IN THE CASCADES

Volcanic ejecta from Mount Rainier, Mount St. Helens (80 km south-southwest of Mount Rainier), and Mount Mazama, Oregon (site of Crater Lake; 440 km south of Mount Rainier) are bracketed by radiocarbon dates, making it possible to assign limiting ages to associated glacial and periglacial deposits (Fig. 1). The mid-Holocene Mount Mazama tephra and two Mount St. Helens tephras were deposited across Mount Rainier. Mount Rainier tephras are mainly restricted to the mountain, and were associated with much smaller eruptions than the cataclysmic eruption of Mount Mazama, which spread tephra across much of the Pacific Northwest and southwestern Canada. The aerial distribution of a Rainier tephra unit was controlled both by the directed trajectory of the explosive eruption and the prevailing wind during the eruption.

Holocene tephra units used in this study, and their ages, were described by Mullineaux (1974) (Fig. 3). Crandell and Miller (1964) and Crandell (1969) used the tephra stratigraphy in their reconnaissance mapping of surficial deposits on Mount Rainier because it provided an excellent basis for establishing bracketing ages for Neoglacial moraines.

2.1.2 IDENTIFICATION AND DATING OF TEPHRA LAYERS

Limiting ^{14}C ages for tephra units used in this project (Fig. 3) are based on organic matter found in and immediately adjacent to the tephra horizons (Mullineaux, 1974). Units identified on Mount Rainier differ in color, mineralogy, thickness, and grain size (Fig. 3), making them easy to identify in the field. Mullineaux's (1974) isopleth and isopach maps show that grain size and thickness of each tephra layer vary mainly with the direction and strength of the wind at the time of an eruption. Brantley et al. (1986), dated tephra unit W using dendrochronology. Tephra units originating from Mt. St. Helens are distinguished from tephras of Mount Rainier by their high silica content and the typical presence of clinopyroxene hornblende. During the initial field reconnaissance for this

project, samples of each tephra were collected for verification with known chemical compositions of each unit (Mullineaux, 1974; Table 1).

Table 1: Tephra Chemical Composition Data (percent)

Mineral	R ¹	O ²	Tephra Layer		
			Yn ²	C ²	W ²
SiO ₂	60.12	68.56	63.4	59.77	67.5
Al ₂ O ₃	18.85	14.22	17.2	17.36	16.2
Fe ₂ O ₃	“	1.42	1.6	1.59	1.3
FeO	6.11	1.49	2.3	3.74	2.1
MgO	2.81	0.83	1.3	3.51	1.0
CaO	5.16	2.35	4.1	5.71	3.6
Na ₂ O	3.83	5.18	4.3	3.97	4.8
K ₂ O	1.70	2.47	1.2	1.71	1.6
H ₂ O-	“	3.32	0.76	0.32	0.1
H ₂ O+	“	3.32	2.3	0.76	1.0
TiO ₂	1.03	0.58	0.51	0.89	0.4
P ₂ O ₅	0.28	0.10	0.17	0.20	0.1
MnO	0.11	0.03	0.08	0.09	0.1
CO ₂	“	0.00	0.05	0.02	0.1

¹Sisson (2003)²Mullineaux (1974)

2.2 SURFACE-EXPOSURE DATING

Surface-exposure dating has gained popularity in the last decade as a tool for determining the exposure histories of various Quaternary landforms (Gosse and Phillips, 2001). This dating method uses isotopes that were produced by exposure of a sampled rock surface to cosmic radiation. The commonly used cosmogenic isotopes include helium (^3He), beryllium (^{10}Be), aluminum (^{26}Al), and chlorine (^{36}Cl). Using surface-exposure dating, the time of a depositional or erosional event can be estimated. For example, determining how long the surface of an unweathered or little-weathered moraine or lahar boulder has been exposed to cosmic radiation, the elapsed time since boulder or lahar deposition can be determined. Also, the exposure age (time since deglaciation) of a glacially eroded bedrock surface can be dated. In this project, the chlorine-36 (^{36}Cl) method was used because Mount Rainier andesite contains calcium (Ca), which is a target element for ^{36}Cl . Since the andesite does not contain enough quartz, ^{10}Be and ^{26}Al are not produced in these rocks.

2.2.1 FACTORS INFLUENCING EXPOSURE AGES

Many factors can influence the amount of radiation that a rock surface receives and, therefore, the isotopes produced.

- 1) A surface receives more radiation with increasing altitude and latitude.
- 2) A rock surface can be shielded from cosmic radiation by high topography near the sampled surface, by trees, soil, the angle of the exposed surface, and by water (including ice or snow).
- 3) Trace elements in the rock (e.g., boron (B), gadolinium (Gd), uranium (U), and thorium (Th)) can influence isotope production through *in situ* production or absorption of incoming neutron flux.

The CHLOE computer spreadsheet program (Chlorine-36 exposure; Phillips and Plummer, 1996), which is used to calculate a surface-exposure age based on field and laboratory data, takes most of these variables into account.

An important factor that often frustrates researchers using the surface-exposure dating method is prior exposure (isotope inheritance) of a boulder or bedrock surface to cosmic radiation. At least 2 m of the surface must be removed by erosion for all cosmogenically produced isotopes from a previous exposure interval to be removed. Otherwise, an anomalously old age for the boulder or bedrock surface may be obtained.

Moraines are susceptible to rapid initial degradation (Hallet and Putkonen, 1994; Putkonen, 2003). A boulder would produce an anomalously young surface-exposure age if it had been buried in sediment and later exhumed (Fig. 4). As a moraine degrades, exhumed boulders are vulnerable to sliding or rolling down the steep moraine slopes. The top surface of a displaced boulder may not have been exposed previously to cosmic radiation, resulting in an anomalously young age. In the case of closely nested moraines, a boulder that has rolled down the proximal slope of one moraine may be mistakenly assigned to an adjacent younger moraine.

Physical and chemical weathering rates of andesitic rock surfaces are generally assumed to be of ca. 0.1 mm/kyr (Bierman et al., 1999). The calculated surface-exposure ages in this study would have to be adjusted if they were greater than ca. 10,000 yr to account for the loss of cosmogenic isotopes due to the weathering and erosion of the Mount Rainier andesite. For this study, the young (Holocene) age of the landforms being dated minimizes this and most other potential uncertainties.

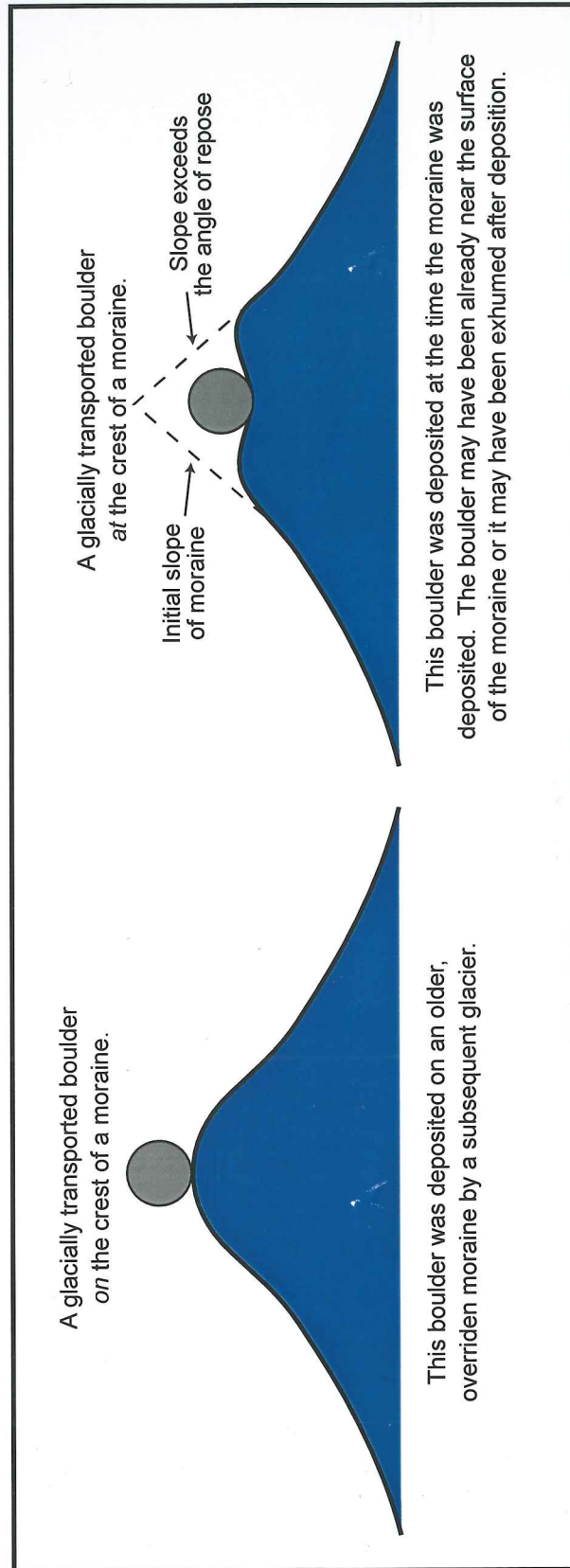


Figure 4: Boulder exhumation explanation. An explanation of the depositional history of boulders found on the crest of a moraine versus at the surface of a moraine.

2.2.2 SAMPLE COLLECTION

Exposed boulders and eroded bedrock surfaces initially identified as Holocene in age based on tephrochronology were sampled to establish a glacial chronology. Moraine boulders were selected for sampling based on their position, size (> 50 cm diameter), height above ground, and exposure to solar radiation. Moraine boulders generally were sampled near the crest of a moraine. More than half of a sampled boulder stood above the soil surface to minimize uncertainty about exhumation. Sampled boulders had minimum shielding ($\leq 30^\circ$; Table 2b) from adjacent high trees or mountain slopes. Most samples (ca. 0.5-1.0 kg) were obtained from near-horizontal surfaces ($< 15^\circ$ slope) at or near the top of a boulder. Only the top 1-3 centimeters of an exposed rock surface was sampled to reduce depth dependence problems (Liu et al., 1994). At each site, 2 to 6 boulders were sampled. One sample was taken from a bedrock surface adjacent to a moraine. The bedrock was sampled much the same way as the boulder. A glacially polished surface that protruded >50 cm from the soil was sampled to minimize uncertainty about the exposure history due to soil cover.

2.2.3 LABORATORY METHODS

Rock samples for ^{36}Cl analyses were prepared using a whole-rock wet chemical procedure described by Zreda et al. (1991) as modified by Swanson (1994). The prepared samples were analyzed using accelerator mass spectrometry (AMS) at the Center for Accelerator Mass Spectrometry (CAMS), Lawrence Livermore National Laboratory, Livermore, California. Major element compositions of the ground whole-rock samples were determined by X-ray fluorescence (XRF) spectrometry. Prompt gamma emission spectrometry was used to determine B and Gd contents of the samples. U and Th compositions of the rock samples were determined by neutron activation. Except for total chlorine, all element compositions were calculated at the XRAL Laboratories, Don Mills, Ontario, Canada, and have an uncertainty of <2%. Total chlorine content of the samples was measured by a combination ion-selective electrode at

the University of Washington. At least three total chlorine measurements were made for each sample to attain an uncertainty of <6%. Initial filtering and analyses of the raw data were performed by Marc Caffee (CAMS).

Data were entered in the CHLOE program (Phillips and Plummer, 1996), which was modified to incorporate the ^{36}Cl production rates determined by Swanson and Caffee (2001). These production rates were used because they were derived from rock surfaces <2° latitude north of Mount Rainier. Error in ^{36}Cl surface-exposure ages arises primarily from the precision of the AMS and the total chlorine measurements of the prepared rock samples (Swanson and Caffee, 2001). Error for each date is based on AMS uncertainty and is ca. $\pm 5\%$ of the surface-exposure age. The total chlorine measurement has an uncertainty of ca. 25% of the AMS uncertainty. Varying estimated snowpack conditions and sample ages for each snowpack condition were calculated. Sample data are listed in Table 2a-e.

Table 2a: Field Data for Surface-Exposure Age Samples

Sample	Collection Date	Altitude (m)	Latitude (degrees)	Longitude (degrees)	Thickness (cm)
PL-1	22-10-99	1735	46.8	122.7	2
PL-2	22-10-99	1790	46.8	122.7	2
PL-3	22-10-99	1780	46.8	122.7	2
PL-4B	22-10-99	1775	46.8	122.7	2
PL-5	22-10-99	1780	46.8	122.7	2
PG-1	10-09-99	1855	46.8	122.7	2
PG-2	10-09-99	1890	46.8	122.7	2
PG-3	10-09-99	1887	46.8	122.7	2
PG-4	10-09-99	1887	46.8	122.7	2
FF-1	09-10-99	1755	46.8	122.7	2
FF-2	09-10-99	1755	46.8	122.7	2
FF-3	09-10-99	1755	46.8	122.7	2
FF-4	09-10-99	1755	46.8	122.7	2
FF-5B	09-10-99	1755	46.8	122.7	2
BP-A	02-10-99	1945	46.8	122.7	2
BP-B	02-10-99	1945	46.8	122.7	2
BP-C	02-10-99	1945	46.8	122.7	2
BP-D	02-10-99	1945	46.8	122.7	2
BP-E	02-10-99	1945	46.8	122.7	2
BP-F	02-10-99	1945	46.8	122.7	2
GC-G	02-10-99	2010	46.8	122.7	2
GC-H	02-10-99	2010	46.8	122.7	2
GC-I	02-10-99	2010	46.8	122.7	2
GC-J	02-10-99	2015	46.8	122.7	2
GC-K	02-10-99	2015	46.8	122.7	2

Table 2b: Shielding¹ Data for Surface-Exposure Age Samples

Sample	Compass Direction							
	N	NE	E	SE	S	SW	W	NW
PL-1	17		14		0		12	
PL-2	17		11		0		2	
PL-3	13		9		1		2	
PL-4B	18		7		1		6	
PL-5	14		9		1		2	
PG-1	10		0		0		5	
PG-2	10		0		0		15	
PG-3	18		14		0		7	
PG-4	18		14		0		7	
FF-1	14	21	18	4	4	2	11	13
FF-2	14	21	18	4	4	2	11	13
FF-3	14	21	18	4	4	2	11	13
FF-4	14	21	18	4	4	2	11	13
FF-5B	14	21	18	4	4	2	11	13
BP-A	11	9	23	30	19	20	10	9
BP-B	11	9	23	30	19	20	10	9
BP-C	11	9	23	30	19	20	10	9
BP-D	10	10	16	28	28	24	13	12
BP-E	10	10	16	28	28	24	13	12
BP-F	10	10	16	28	28	24	13	12
GC-G	0	5	10	12	16	20	9	0
GC-H	0	5	10	12	16	20	9	0
GC-I	0	5	10	12	16	20	9	0
GC-J	0	5	10	12	16	20	9	0
GC-K	0	5	10	12	16	20	9	0

¹Angle (degrees) from rock surface to the top of surrounding land surface

Table 2c: Total Chlorine Data for Surface-Exposure Age Samples

Sample	Average	Standard	Percent	Total Chlorine		
	Total Chlorine (ppm)	Deviation	Error	Measurements (ppm)		
PL-1	266	11.0	4.9	237	227	215
PL-2	32	1.5	4.8	33	32	30
PL-3	94	4.4	4.6	89	97	96
PL-4B	105	5.1	4.9	109	106	99
PL-5	187	6.7	3.6	195	183	184
PG-1	341	6.6	1.9	348	340	335
PG-2	110	4.4	4.0	105	112	113
PG-3	277	14.0	5.1	261	283	287
PG-4	36	1.2	3.2	37	37	35
FF-1	290	16.5	5.7	301	298	271
FF-2	35	1.5	4.4	33	36	35
FF-3	170	9.1	5.3	179	171	160
FF-4	221	13.1	5.9	231	206	225
FF-5B	32	1.5	4.8	33	30	32
BP-A	30	3.1	10.1	33	27	31
BP-B	37	1.2	3.1	38	36	36
BP-C	34	1.2	3.4	33	35	33
BP-D	34	1.0	2.9	34	33	35
BP-E	32	1.7	5.4	33	30	33
BP-F	32	0.6	1.8	32	33	32
GC-G	51	1.2	2.2	52	52	50
GC-H	83	2.6	3.2	84	80	85
GC-I	26	1.5	5.8	25	26	28
GC-J	26	1.5	5.8	28	25	26
GC-K	41	2.1	5.0	42	43	39

Table 2d: Elemental Oxide Composition Data for Surface-Exposure Age Samples

Sample	Oxides (percent of total rock)										
	CO ₃	Na ₂ O	MgO	Al ₂ O ₃	SiO ₂	P ₂ O ₅	K ₂ O	CaO	TiO ₂	MnO	Fe ₂ O ₃
PL-1	0	3.8	2.8	16.2	63	0.2	1.8	4.7	0.83	0.1	5.45
PL-2	0	4.0	2.7	16.9	63	0.2	1.6	5.1	0.77	0.1	5.11
PL-3	0	4.0	3.3	16.3	62	0.2	1.7	5.4	0.80	0.1	5.82
PL-4B	0	4.2	2.9	19.7	62	0.2	1.8	5.2	0.80	0.1	5.81
PL-5	0	4.0	3.5	16.5	62	0.3	1.6	5.0	0.82	0.1	5.47
PG-1	0	3.9	2.9	16.2	61	0.2	2.1	5.4	0.86	0.1	5.68
PG-2	0	4.0	2.8	15.9	64	0.2	2.0	4.7	0.79	0.1	5.41
PG-3	0	4.1	3.6	16.9	61	0.1	1.6	6.0	0.87	0.1	5.95
PG-4	0	4.2	3.0	16.1	63	0.0	2.1	4.9	0.79	0.1	5.12
FF-1	0	4.0	3.0	16.3	62	0.1	2.3	5.4	0.87	0.1	5.68
FF-2	0	4.1	2.9	16.2	63	0.0	1.9	5.0	0.70	0.1	5.04
FF-3	0	4.0	3.4	16.7	60	0.1	2.0	5.9	0.89	0.1	6.17
FF-4	0	4.0	3.3	16.5	60	0.1	2.3	5.9	0.96	0.1	6.18
FF-5B	0	4.0	3.1	16.3	62	0.1	1.9	5.0	0.80	0.1	5.68
BP-A	0	4.1	3.7	16.7	60	0.1	1.6	5.9	0.86	0.1	6.23
BP-B	0	3.7	3.7	15.3	61	0.1	1.4	5.5	0.83	0.1	6.00
BP-C	0	3.8	3.9	15.9	60	0.1	1.5	5.7	0.90	0.1	6.45
BP-D	0	4.3	3.0	16.5	62	0.1	1.7	5.3	0.78	0.1	5.50
BP-E	0	4.0	2.9	16.4	63	0.1	1.5	5.2	0.79	0.1	5.43
BP-F	0	4.2	2.9	16.2	63	0.1	1.7	5.1	0.77	0.1	5.26
GC-G	0	4.2	3.5	16.7	61	0.1	1.5	5.6	0.85	0.1	6.18
GC-H	0	3.9	3.3	16.3	62	0.1	1.3	5.5	0.78	0.1	5.67
GC-I	0	3.8	3.2	16.3	62	0.1	1.2	5.4	0.79	0.1	5.69
GC-J	0	4.3	3.3	17.1	61	0.1	1.5	5.6	0.82	0.1	5.95
GC-K	0	4.2	3.2	16.8	61	0.1	1.6	5.4	0.81	0.1	5.86

Table 2e: Element Concentration Data for Surface-Exposure Age Samples

Sample	Element (ppm)					
	Cl	B	Gd	Sm	U	Th
PL-1	249	22	0.5	1	2.6	6.6
PL-2	36	11	0.5	1	0.0	0.0
PL-3	103	16	0.5	1	0.0	0.0
PL-4B	94	17	1.0	1	0.0	0.0
PL-5	176	24	0.5	1	0.0	0.0
PG-1	360	20	0.5	1	3.2	7.2
PG-3	305	17	0.5	1	0.0	0.0
PG-4	56	18	0.5	1	0.0	0.0
FF-1	277	23	2.0	2	4.1	12
FF-2	35	14	0.5	1	0.0	0.0
FF-3	170	21	0.5	1	0.0	0.0
FF-4	205	16	2.0	2	0.0	0.0
FF-5B	292	22	0.5	1	0.0	0.0
BP-A	31	11	0.5	1	1.5	3.6
BP-B	30	14	4.0	4	0.0	0.0
BP-C	31	10	2.0	2	0.0	0.0
BP-D	32	14	1.0	1	1.8	5.0
BP-E	32	13	0.5	1	0.0	0.0
BP-F	35	16	0.5	1	0.0	0.0
GC-G	26	10	0.5	1	2.0	3.2
GC-H	50	16	0.5	1	0.0	0.0
GC-I	101	13	1.0	1	0.0	0.0
GC-J	27	7	0.5	1	0.0	0.0
GC-K	38	17	0.5	1	0.0	0.0

2.3 EFFECT OF SEASONAL AND PERENNIAL SNOWPACKS ON COSMOGENIC-ISOTOPE AGES

In areas with significant snow accumulation, previous studies using surface-exposure ages to date landforms have estimated the shielding effect of snow on the calculated ages (e.g., Gosse et al., 1995). The greatest uncertainty when attempting to obtain relatively young ^{36}Cl surface-exposure ages on Mount Rainier is the thick, dense annual snowpack that mantles the mountain for at least nine months each year. Snowpacks up to 9 m thick have been reported at Paradise Ranger Station (Plate 1; Table 3), where annual snowfall of >30 m has been recorded during exceptional years. The thick annual snowpack shields exposed rock surfaces at the altitude of Holocene moraines from cosmic rays, affecting the reliability of surface-exposure dates. Calibration of sampled glacially eroded bedrock and boulders of known exposure age is required to determine the shielding effect of a thick, dense annual snowpack at an altitude of ~1750 m on Mount Rainier. The calibration sites should be in a similar climate and at a similar altitude as moraine rock surfaces to be dated.

An area of the Paradise Lahar deposit (Crandell and Miller, 1964) above Paradise Ranger Station was selected as a calibration site (Plate 1 and Fig. 5) because of the large (>2-m-diameter) boulders at the surface of the lahar and their relatively unrestricted exposure to cosmic radiation. Sampled lahar boulders lie within 100 m altitude and <2 km distance from two of the four field sites in this project (Plate 1). The Paradise Lahar has been independently dated using the radiocarbon method. The ten radiocarbon dates in Table 4 are from samples of the Paradise Lahar and the contemporaneous Osceola Lahar (Vallance and Scott, 1997).

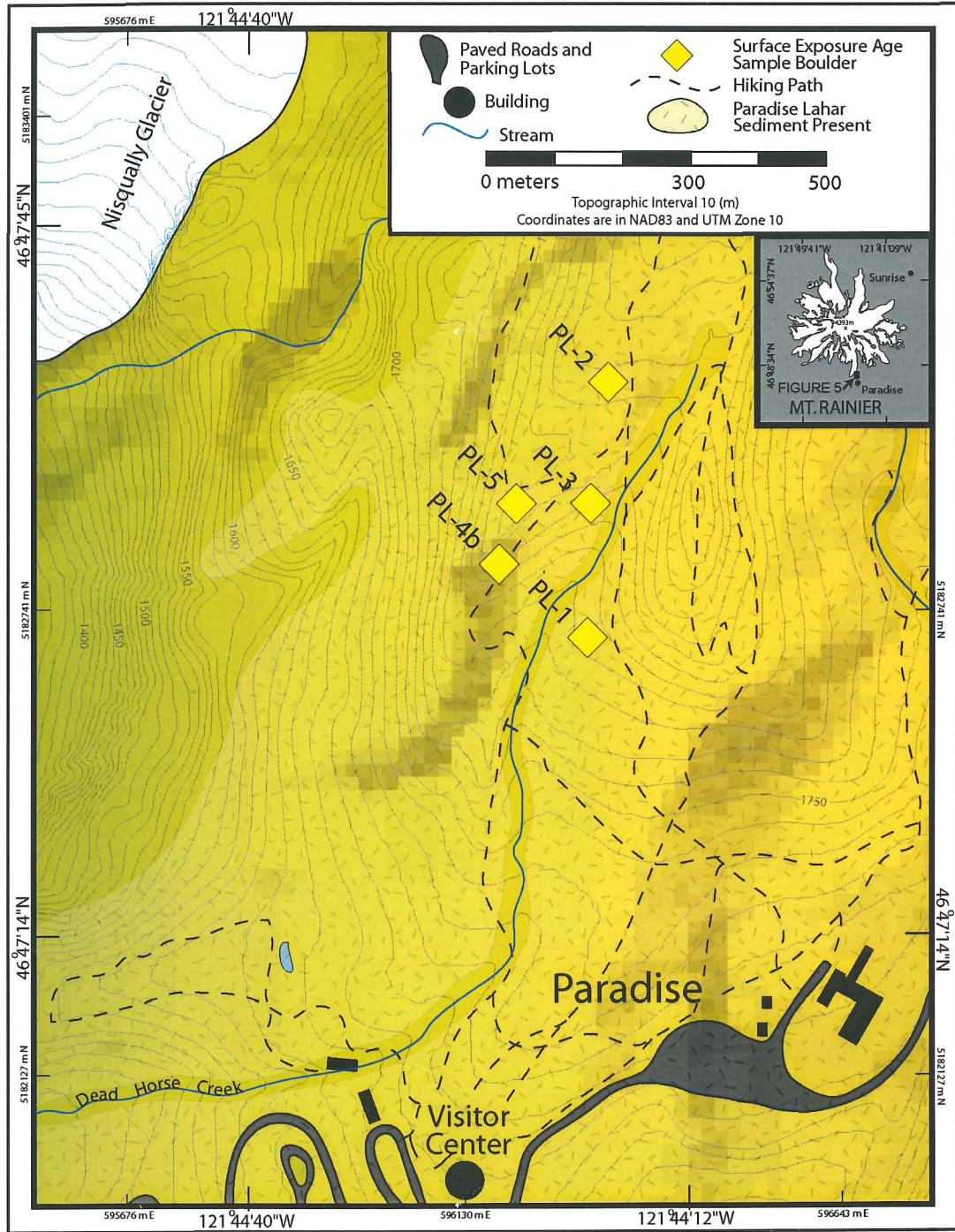


Figure 5: Map of Paradise Lahar calibration site. The map shows Paradise Lahar surface-exposure sample localities in relation to the Paradise Park Visitors Center and Nisqually Glacier.

**Table 3: Snowpack Thickness (m) Measured Annually on March 15
at Paradise Ranger Station, Mount Rainier¹**

Year	Thickness	Year	Thickness	Year	Thickness	Year	Thickness
1916	5.08	1939	5.79	1965	4.34	1988	4.07
1917	6.00	1940	2.95	1966	4.65	1989	4.55
1918	4.57	1941	2.06	1967	5.23	1990	4.73
1919	6.30	1942	2.67	1968	2.59	1991	4.27
1920	3.46	1943	4.14	1969	6.00	1992	3.02
1921	5.49	1944	2.67	1970	3.46	1993	3.10
1922	4.67	1945	3.76	1971	6.89	1994	3.25
1923	5.89	1946	5.87	1972	6.81	1995	4.24
1924	4.27	1947	4.70	1973	3.07	1996	2.90
1925	5.59	1948	5.03	1974	6.81	1997	6.55
1926	2.79	1951	5.03	1975	5.08	1998	4.22
1927	5.03	1953	4.50	1976	4.98	Mean	4.4 ± 1.3(1σ)
1928	3.20	1954	5.34	1977	2.85	Maximum	9.07
1929	4.37	1955	5.11	1978	3.81	Minimum	1.8
1930	2.57	1956	9.07	1979	3.51		
1931	2.59	1957	4.67	1980	4.07		
1932	5.08	1958	4.14	1981	1.83		
1933	5.49	1959	4.52	1982	5.49		
1934	2.54	1960	3.94	1983	4.17		
1935	4.04	1961	5.34	1984	4.07		
1936	4.98	1962	3.86	1985	3.86		
1937	4.42	1963	2.31	1986	5.49		
1938	3.73	1964	5.67	1987	3.76		

¹ Ebbesmeyer and Strickland (1995)

**Table 4: Radiocarbon Dates Associated with the
Osceola and Paradise lahars**

Age (^{14}C yr BP)	Age (cal yr BP) ²	Source
4455 ± 355 ³	5580-4623	*Wood from basal 50 cm of Osceola Lahar at Huckleberry Creek
4625 ± 240 ³	5588-4983	*Charcoal in Paradise Lahar at Ricksecker Point
4700 ± 250 ¹	5658-5043	*Wood in Osceola Lahar
4730 ± 320 ³	5855-4976	*Charcoal from upper part of Paradise Lahar at National
4800 ± 300 ¹	5899-5059	*Wood in Osceola Lahar
4950 ± 300 ¹	6164-5318	*Wood in Osceola Lahar
4955 ± 585 ³	6301-4879	Wood from just above Layer O and below Paradise Lahar at Longmire
4980 ± 200 ³	5937-5477	Wood from upper glaciofluvial deposit below Osceola Lahar at Huckleberry Creek
5040 ± 150 ¹	5919-5616	*Wood in Osceola Lahar
5230 ± 235 ³	6273-5745	Charcoal above Layer O and below two pre-Osceola lahars near Buck Creek
Mean = 4757 ± 197 ^{14}C yr BP		
Mean 1σ calibrated age = 5078-5074 cal yr BP ²		

*sample used for calculating mean age of lahars

¹Crandell (1971)

²Stuvier et al. (1998)

³Vallance and Scott. (1997)

Near the Paradise Ranger Station, the lahar deposit has not been overridden by a glacier since it was deposited (Fig. 5). Surfaces of lahar boulders are presumed to lack inherited ^{36}Cl isotopes. Mullineaux (1974, p. 19) asserted that the Osceola Lahar, and thus the Paradise Lahar, were caused by a "phreatic explosion that caused a large part of the former summit to avalanche and form the lahar." It is unlikely that an exposed rock surface at or near the summit descended >2000 m to the area of the Paradise Ranger Station to be deposited with the previously exposed surface facing upward.

Snowpack estimates are based on historic records that extend back to 1916. Mean annual snow depth on March 15 for the 80 years of record at Paradise Ranger Station (1650 m) is 4.40 m (Ebbesmeyer and Strickland, 1995) (Table 3). A study of perennial snowpatches on Mount Rainier by Frederick (1980) used late-summer aerial photographs covering the Paradise Lahar calibration site and Paradise Glacier field site (Plate 1). She mapped perennial snowpatches from the photographs, spanning a 23-year period. During at least 5 of the 23 years, both field sites were covered by considerably more perennial snow than during the 1999 field season. In the present study it is assumed that the prehistoric Holocene (i.e., Neoglacial) snowpack thickness also had a range of 4.4 ± 1.0 m.

The CHLOE program (Phillips and Plummer, 1996) allows input of mean monthly snowpack thickness and mean monthly snowpack density to correct for the shielding affect of snow (Table 5). However, the program does not allow for variation in these parameters over the exposure period of the sample. For example, although precipitation and temperature varied throughout Neoglacial time, for a sample with an exposure age of 5000 ^{36}Cl yr, a mean snowpack thickness and density for the month of January remains constant in the CHLOE program over those 5000 ^{36}Cl years. Furthermore, because precipitation varies from the southern side of the mountain to the northern side, the error resulting from snowpack estimates is greater than all experimental sources of error.

Table 5: Estimated Minimum and Maximum Annual Snowpack Data¹

Month	Minimum Snow Depth (m)	Minimum Equivalent Water Depth (m)	Maximum Snow Depth (m)	Maximum Equivalent Water Depth (m)
January	6	0.08	7	0.09
February	6	0.08	12	0.15
March	6	0.08	12	0.15
April	6	0.08	12	0.15
May	4	0.05	8	0.10
June	3	0.04	5	0.06
July	3	0.04	1	0.01
August	2	0.03	0	0.00
September	3	0.04	0	0.00
October	3	0.04	1	0.01
November	4	0.05	4	0.05
December	5	0.06	6	0.08

¹An average annual snow density of 0.5 is assumed (Ebbesmeyer and Strickland, 1995).

Because Mount Rainier has a precipitation shadow (the southwest side of the mountain receives more annual snow than the northeast side), shielding due to snow cover likely varies across the mountain. To assess this inference, two ages were calculated from the uncorrected ages, one with a minimum estimate of average snowpack thickness, and the other with a maximum estimate of snowpack thickness (Table 5). The minimum and maximum snowpack thickness values were higher for sites on the southwest side of the mountain than for those in the precipitation shadow on the northeast side. A mean annual snow density of 0.5 was used for both estimates on each side of the mountain (Ebbesmeyer and Strickland, 1995). This method also simultaneously allows the range of ages resulting from the inferred range of average annual snowpack to be determined.

The mean calibrated age range (1σ) of the Paradise Lahar from the radiocarbon ages in Table 4 is 5078-5074 cal yr BP. The five samples taken from the calibration site on the Paradise Lahar show how dramatically young (ca. 50% younger) the surface-exposure ages are when shielding due to the snowpack is not taken into account (Table 6; Fig. 6). The mean correction value for the five surface-exposure ages at the Paradise Lahar site is 2600 years. The same correction can be directly applied to samples taken from nearby moraines that have limiting tephrochronologic ages as old as the 5550 cal yr BP age of the Paradise Lahar. The potential error of the calibrated ages rises as the exposure ages become older than 5550 cal yr BP because of the need to estimate mean snowpack thickness over a longer time. During the warmer early to middle Holocene (ca. 11,000 – 5500 cal yr BP) snowpacks likely were thinner.

An attempt to calibrate the relatively young surface-exposure ages using historical and inferred snowpack data, and calibration samples of known age (i.e., ^{14}C -dated wood from the lahar), produces ages that usually are not consistent with the tephrochronology. The local consequences of this disagreement will be discussed for each of the field sites.

Ideally, to refine the shielding effect of snow more precisely, a variable average annual snowcover would be used in the surface-exposure age calculation. Further study and modeling is needed, varying average annual snowcover with time according to known local climatic variations, such as those described by fossil pollen and tree-ring records. Surface-exposure ages from areas having a significant annual snowpack are provisional until an accurate method of estimating the long-term shielding effect of the snowpack is determined.

**Table 6: ^{36}Cl Surface-exposure Ages¹
for Paradise Lahar Boulders**

Sample	Uncorrected Age ² (^{36}Cl yr)	Minimum Snowpack ³	Maximum Snowpack ³
		Depth Age (^{36}Cl yr)	Depth Age (^{36}Cl yr)
PL-1	2600 ± 160	5400 ± 340	5520 ± 350
PL-2	1840 ± 120	3800 ± 240	3880 ± 240
PL-3	3220 ± 200	5850 ± 370	6580 ± 410
PL-4b	2810 ± 180	6310 ± 400	6040 ± 380
PL-5	2540 ± 160	6350 ± 350	5770 ± 330
Mean	2600	5540	5560

¹The ages reported are for no erosion and include 1 σ error.

²All ages are rounded to the nearest decade.

³The snowpack has a mean annual density of 0.5 (Ebbesmeyer and Strickland, 1995). An explanation of this value is given in Section 2.4.

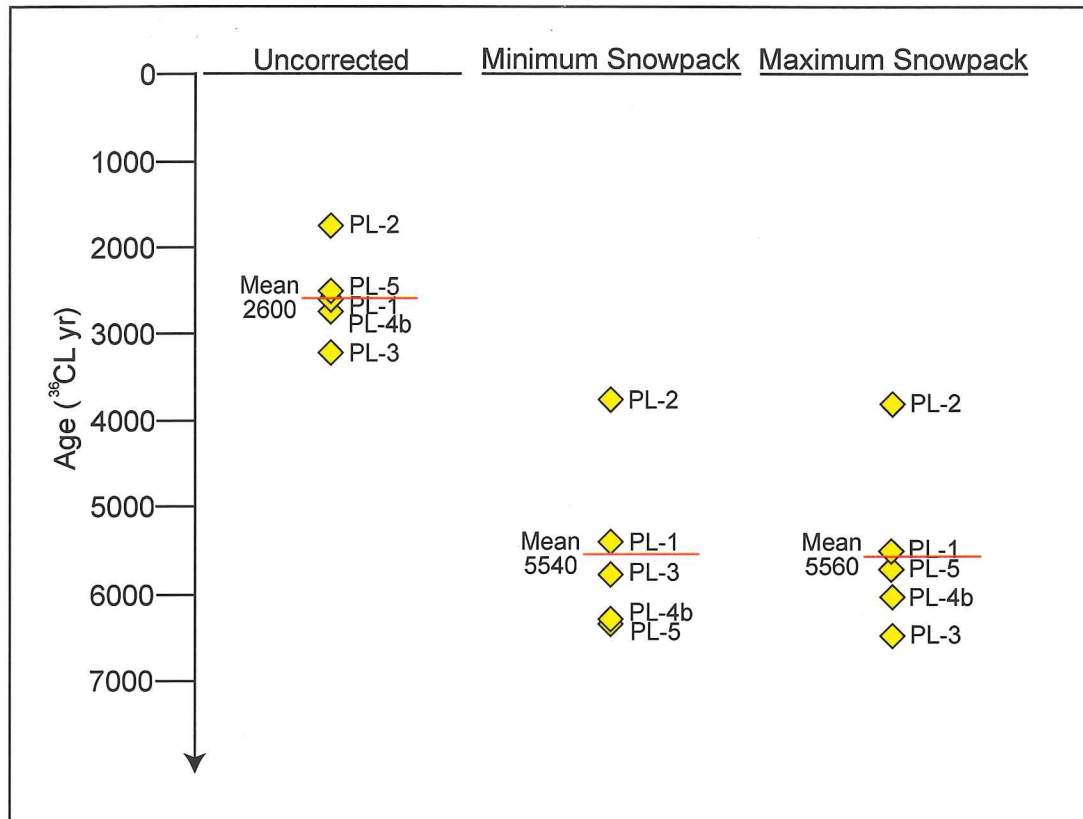


Figure 6: Graph of Paradise Lahar surface-exposure ages. The graph shows uncorrected and snowpack-corrected surface-exposure ages for the Paradise Lahar boulder samples.

3. HOLOCENE GLACIAL RECORD ON MOUNT RAINIER

3.1 FIELD AREA

In selecting suitable sites for this project, aerial photographs of Mount Rainier at a scale of 1:2000 were studied. Candidate sites were selected based on moraine preservation, altitude, and snow cover. Sites were also selected based on their relation to tephra distribution; sites on the western side of the mountain were excluded due to the general absence of tephra units. Sites also were eliminated when an initial field inspection indicated absence of tephra or an unusually thick snow cover. Four sites met the basic criteria: Paradise Glacier and Fairy Falls on the southern side of the mountain, and Granite Creek and Berkeley Park on the northeastern side of the mountain (Plate 1).

Moraines were mapped on enlarged U.S. Geological Survey 7.5-minute topographic quadrangle maps and on aerial photographs. Pits were dug on the crests, between, in front of, and behind each moraine at each site to determine the local tephra stratigraphy (Fig. 3). Taluses with interstratified tephra units in the vicinity of the Paradise Glacier field site were also mapped and described to assess whether episodes of talus construction were correlative with times of glacier advance.

3.2 PARADISE GLACIER SITE

Ten moraine segments were mapped at the Paradise Glacier field site (Fig. 7). Six of the segments are older than 7650 cal yr BP (>6800 ^{14}C yr BP), as they are overlain by tephra layer O. Two moraine segments have ages between 2200 (layer C) and 3400 (layer Yn) ^{14}C yr. The remaining two segments have an age of greater than 1480 A. D. (younger than layer W).

Four samples for surface-exposure dating were collected at the Paradise site (Figs. 7 and 8). Three sampled boulders were ~ 0.5 m in diameter. Sample PG-1 was from the only

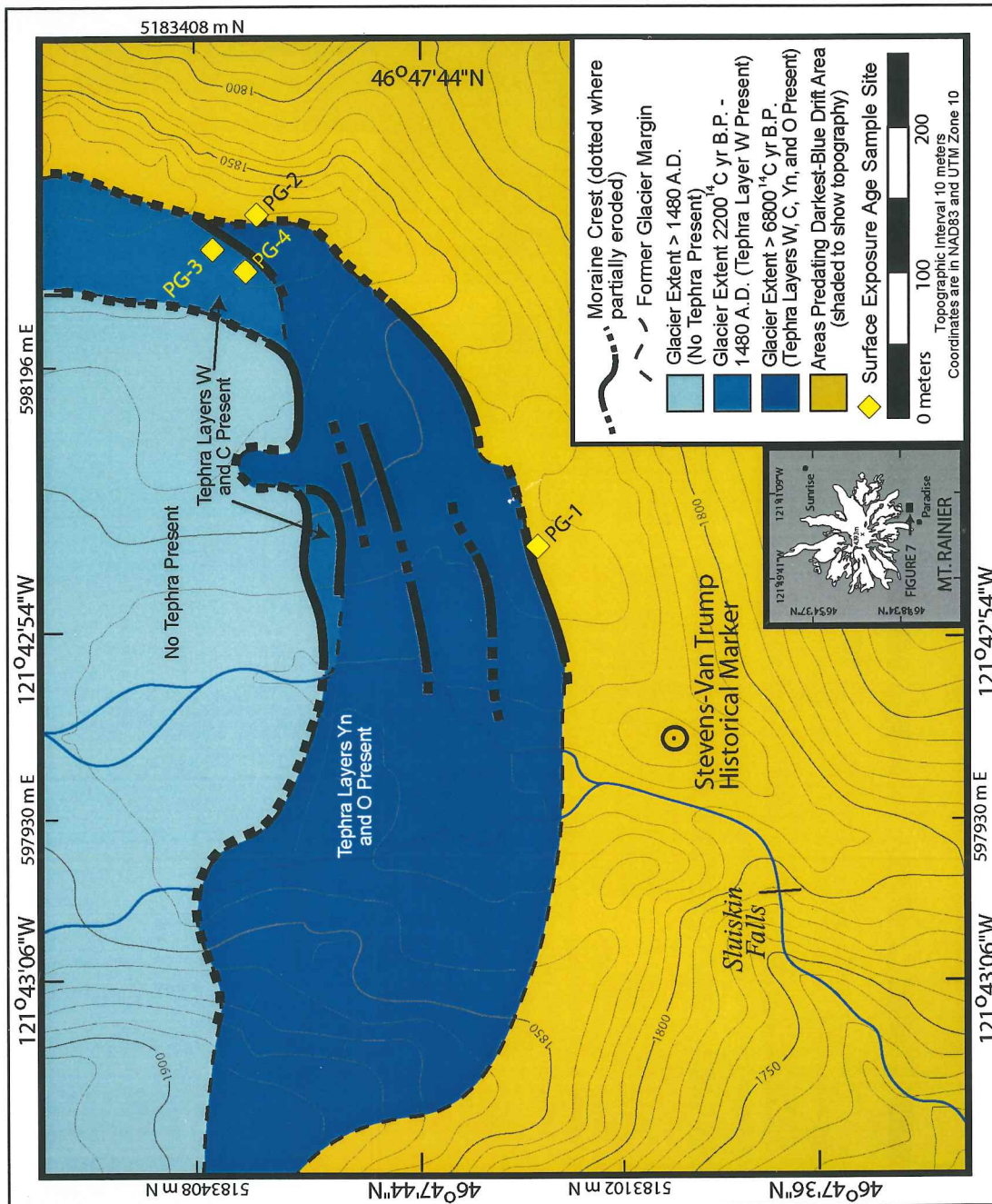


Figure 7: Map of the Paradise field site. The map shows locations of moraines, former extent of Paradise Glacier, tephra units, and surface-exposure sample localities at the Paradise Glacier site.

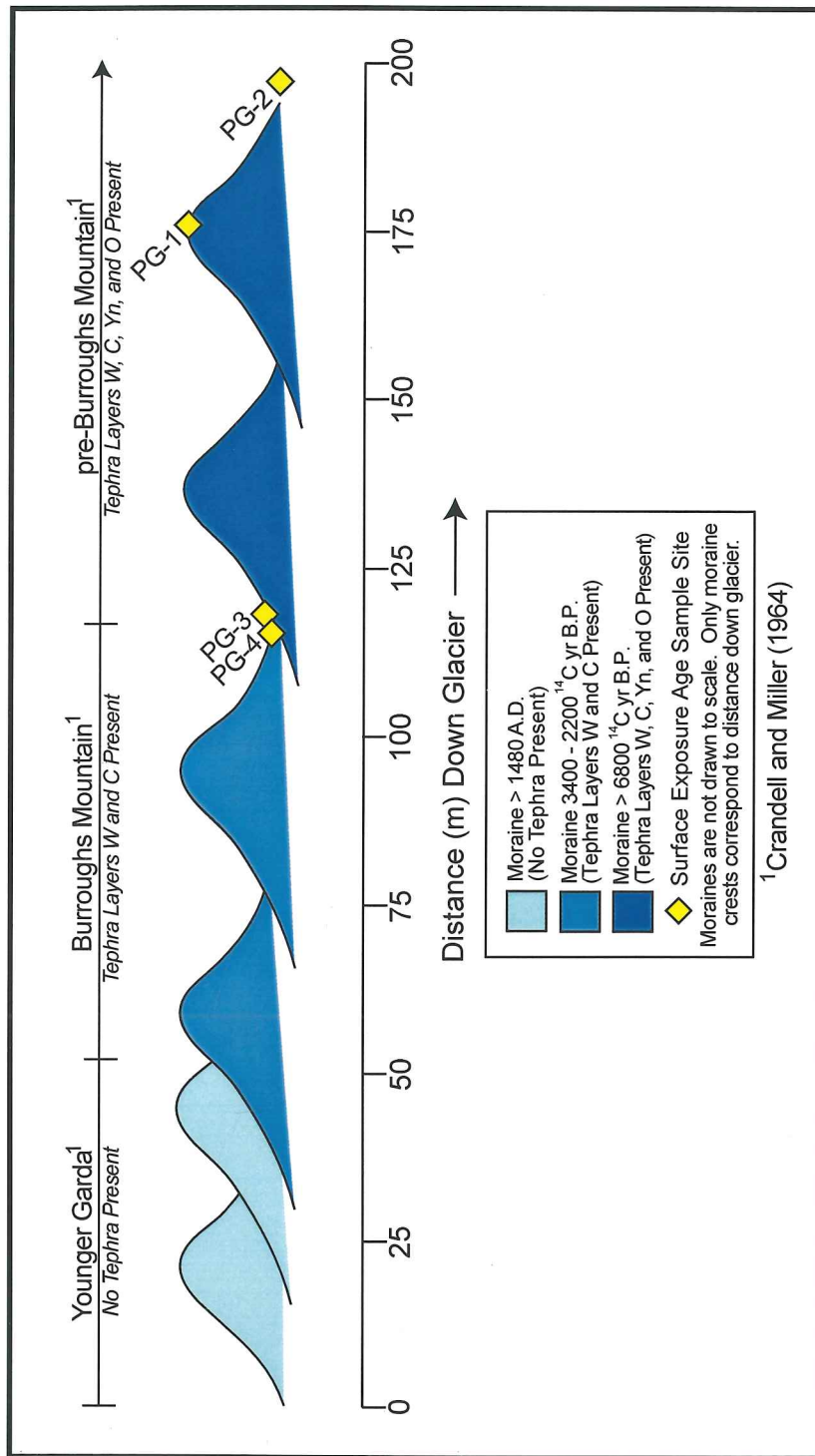


Figure 8: Profile of Paradise Glacier moraines with surface-exposure age sample locations. A diagrammatic profile across the moraines of Paradise Glacier, showing tephrochronologic limiting ages and surface-exposure sample locations.

boulder on the crest of the outermost moraine (>7650 cal yr BP) that met the sampling criteria. PG-2 is from a bedrock surface that is glacially striated and adjacent to the distal slope of the outermost moraine. Sample site PG-2 also is at the edge of a steep ~300-m-high cliff lined with small tors having relief of >2 m. The small tors of hard Rainier Andesite lie beyond the mapped Holocene glacier limit. The snowpack-calibrated ages of the surface suggest that the last time glacier ice covered the surface was in late full-glacial or early late-glacial time (i.e., 17,350-15,670 ^{36}Cl yr ago). To the northeast, the moraine segment is truncated by an intersecting cliff. Samples PG-3 and PG-4 are from the only other boulders on or near the outermost moraine that met the sampling criteria. These two boulders lie in a trough between the outermost moraine and an inner, adjacent moraine, raising the possibility that the boulders might actually be associated with either moraine.

**Table 7: ^{36}Cl Surface-exposure Ages¹
for the Paradise Field site**

Sample	Uncorrected Age ² (^{36}Cl yr)	Minimum Snowpack ³ Depth Age (^{36}Cl yr)	Maximum Snowpack ³ Depth Age (^{36}Cl yr)	Tephro- chronologic Age of Moraine at Sample Site (^{14}C yr)
PG-1	5620 ± 530	12,870 ± 1210	14,180 ± 1330	>6800
PG-2	6540 ± 380	15,670 ± 900	17,350 ± 1000	>6800
PG-3	560 ± 70	1540 ± 200	1350 ± 170	3400-2200
PG-4	470 ± 30	1300 ± 90	1200 ± 80	3400-2200

¹The ages reported are based on an assumption of no erosion and include 1 σ error.

²Rounded to the nearest decade.

³The snowpack has a mean annual density of 0.5 (Ebbesmeyer and Strickland, 1995). An explanation of this value is given in Section 2.4.

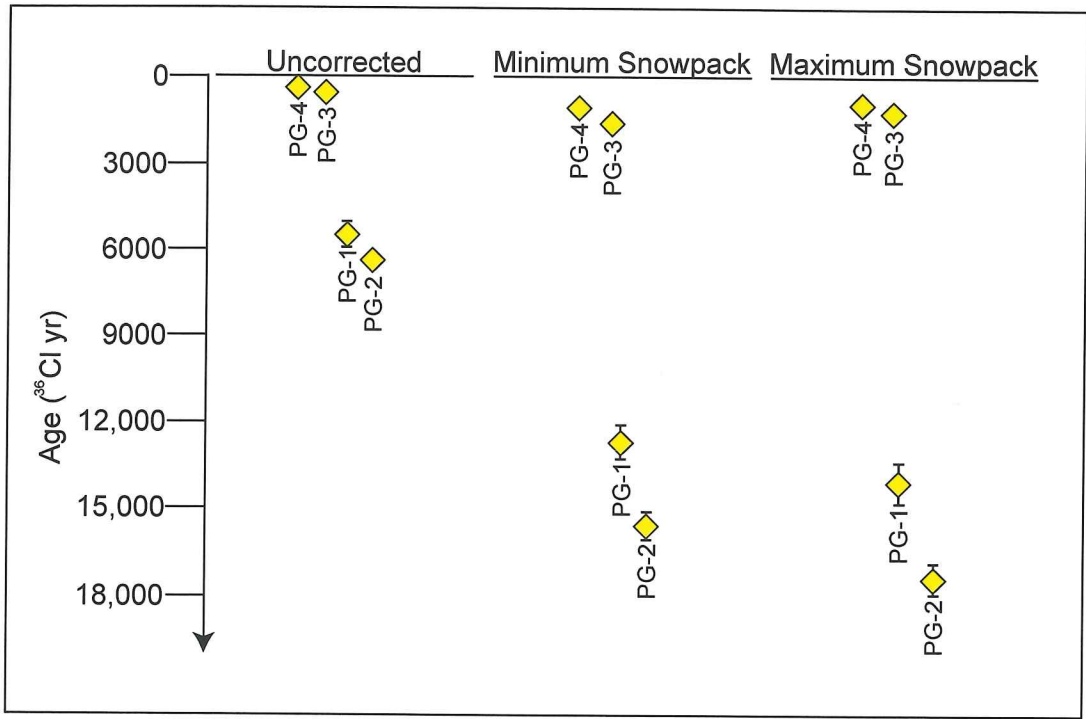


Figure 9: Graph of Paradise Glacier surface-exposure ages. Graph of uncorrected and snowpack-corrected surface-exposure ages with 1-sigma error bars (error encompassed by symbol when not shown) for the Paradise Glacier site samples.

The corrected surface-exposure age of 14,180-12,870 ^{36}Cl yr BP (Table 7; Fig. 9) implies that this moraine formed during McNeely 1 time (Heine, 1997). Tephra layer O provides only a minimum limiting age, allowing either a late-glacial or early-Holocene age for the moraine. The outermost moraine likely represents a halt or readvance of the glacier, although with only a minimum limiting tephrochronologic age it is possible that it is a McNeely moraine. Moraines with last-glacial-maximum (LGM) age, or late-glacial age, like the snowpack-calibrated ages of PG-1, should be found at a lower altitude on Mount Rainier (i.e., related to a much-lower snowline) unless this moraine segment represents a high-altitude late-glacial recessional moraine.

Sample sites PG-3 and PG-4 lie between two moraine segments and their ages are bracketed between those of the O and C tephtras. The two boulders have exposure ages too young to be consistent with the tephrochronology. Both snowpack-calibrated ages fall between 1550 and 1200 ^{36}Cl yr BP. These ages suggest that these two moraines date to a pre-LIA advance. Based on tephrochronology, the two segments have a late middle Neoglacial age and correspond to Crandell and Miller's (1964) Burroughs Mount Drift. A moraine of this age is consistent with Crandell's (1969) reconnaissance mapping of this area. The anomalously young exposure ages of the boulders may have been caused by the boulders rolling from the crest of either moraine segment well after deposition or by exhumation of the boulders, thereby exposing a fresh rock surface to cosmic radiation. It is also possible that snow can remain for a longer time in the protected trough between the two moraines where the PG-3 and PG-4 boulders were found. If correct, however, the young exposure ages imply an error in the tephrochronologic age of the moraine, possibly placing it between tephra layers C and W. It is also possible that the snowpack calibration values do not work for surfaces as young as PG-3 and PG-4 (late Neoglacial). This implies that the assumed climatic history used to predict an average annual snowpack over the 5500 cal yr history of the calibration boulder surfaces will need to be further refined for calibrating surfaces of younger age.

The innermost two moraine segments beyond Paradise Glacier lack tephra or datable boulders. The absence of tephra unit W means that they < 524 yr old. This age corresponds to Crandell's (1969) Younger Garda Drift, which is a LIA deposit. No deposits corresponding to Crandell's (1969) Older Garda Drift (ca. 2200 ¹⁴C yr – 1480 A.D.) were seen at this site, unless the tephrochronologic age of the moraine below samples PG-3 and PG-4 is incorrect.

A profile of Paradise Glacier (Fig. 10) at the time the outermost moraine was built is based on the position of the end moraine, remnants of lateral moraines, and glacially eroded bedrock upglacier from the terminus (Fig. 7). A map of the full extent of Paradise Glacier at the time these moraines were deposited is shown in Figure 11 together with glacier-surface contours and equilibrium line altitudes (ELA) (Sec. 4).

3.3 WILLIWAKAS GLACIER/FAIRY FALLS SITE

Williwakas Glacier built the moraines at Fairy Falls (Fig. 12). Its accumulation area lies just east of that of Paradise Glacier (Fig. 11). Four moraine segments were mapped at the Fairy Falls site. Based on the tephrochronology, the outermost segment has an age of >7650 cal yr BP (6800 ¹⁴C yr BP) because it is overlain by tephra layer O. Tephra layer R was not found at the Paradise Glacier and Fairy Falls sites, both on the south flank of the mountain. The next-younger moraine segment has an age between ca. 3650 (layer Yn) and 2225 (layer C) cal yr BP (3400 and 2200 ¹⁴C yr BP). Based on the tephrochronology, the next two segments have ages between 2200 ¹⁴C yr BP and 1480 A.D. and the innermost moraine segment lacks tephra and is <524 yr old.

The four samples (FF-1 – FF-4) in Table 8 and Figure 13 were taken from boulders ≥ 0.75 m in diameter from of the outermost two moraines to determine surface-exposure ages (Fig. 12 and 14). These two moraines have crests standing ca. 1.5 m above the surrounding land surface; the crests are ca. 10 m apart. The low height of the moraines

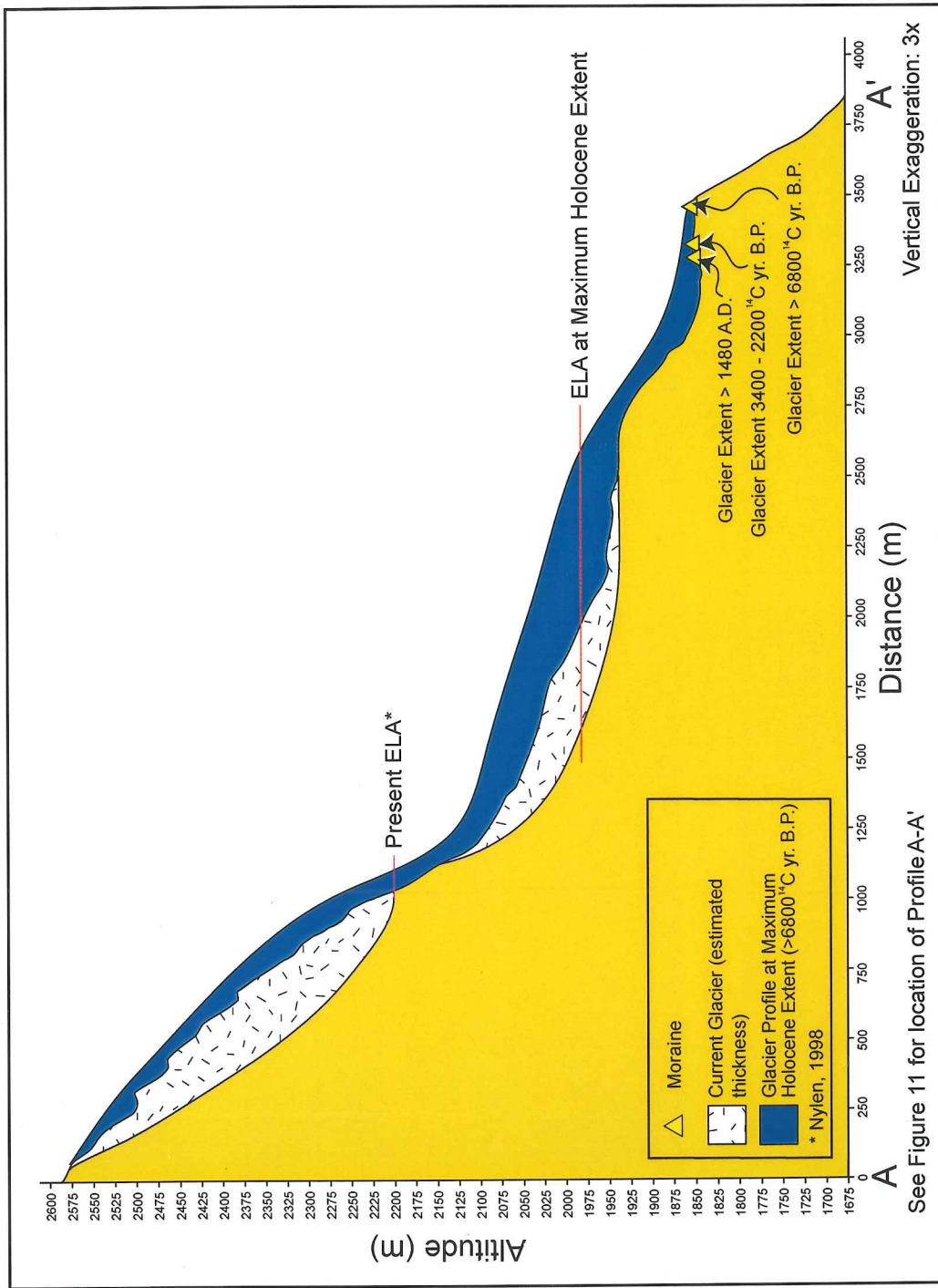


Figure 10: Profile of the glacier that deposited the Paradise moraines. A long profile of Paradise Glacier, showing paleo-ELA, at the time when the outermost moraine at the Paradise Glacier site was deposited.

means that the boulders sampled would experience the maximum shielding of the average 4-m-thick snowpack.

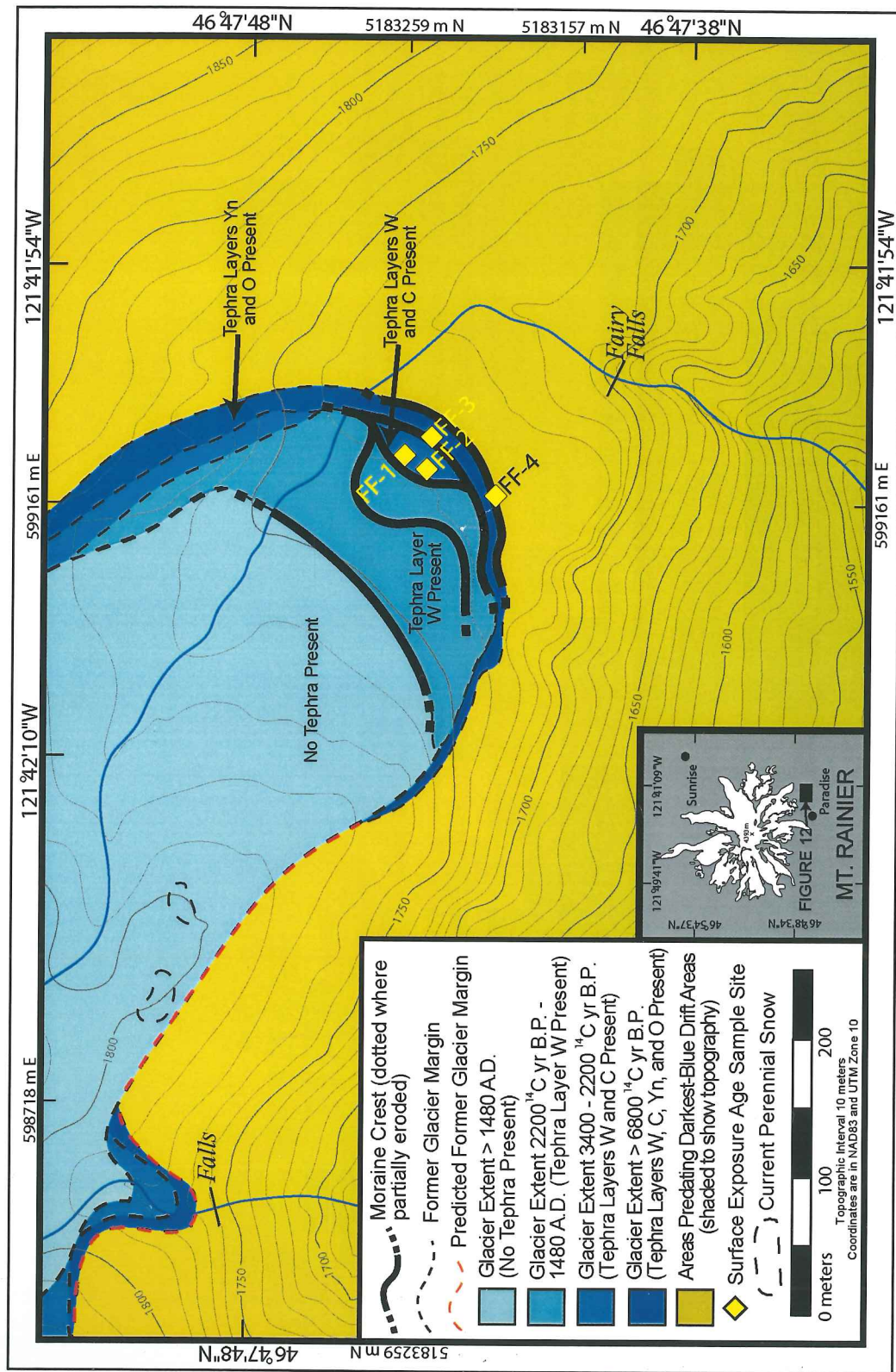


Figure 12: Map of the Williwakas Glacier/Fairy Falls field site. The map shows the location of moraines and extent of former Williwakas Glacier, tephra units, and surface-exposure sample localities for the Fairy Falls site.

**Table 8: ^{36}Cl Surface-exposure Ages¹
for the Fairy Falls field site**

Sample	Uncorrected Age ² (^{36}Cl yr)	Minimum Snowpack ³ Depth Age (^{36}Cl yr)	Maximum Snowpack ³ Depth Age (^{36}Cl yr)	Tephro- chronologic Age of Moraine at Sample Site (^{14}C yr)
FF-1	670 ± 40	1700 ± 100	1550 ± 90	3400-2200
FF-2	1570 ± 400	3700 ± 940	3470 ± 880	3400-2200
FF-3	1560 ± 30	4120 ± 70	3630 ± 70	>3400
FF-4	1060 ± 80	2480 ± 190	2310 ± 170	>6800

¹The ages reported are based on an assumption of no erosion and include 1σ error.

²Rounded to the nearest decade.

³The snowpack has a mean annual density of 0.5 (Ebbesmeyer and Strickland, 1995). An explanation of this value is given in Section 2.4.

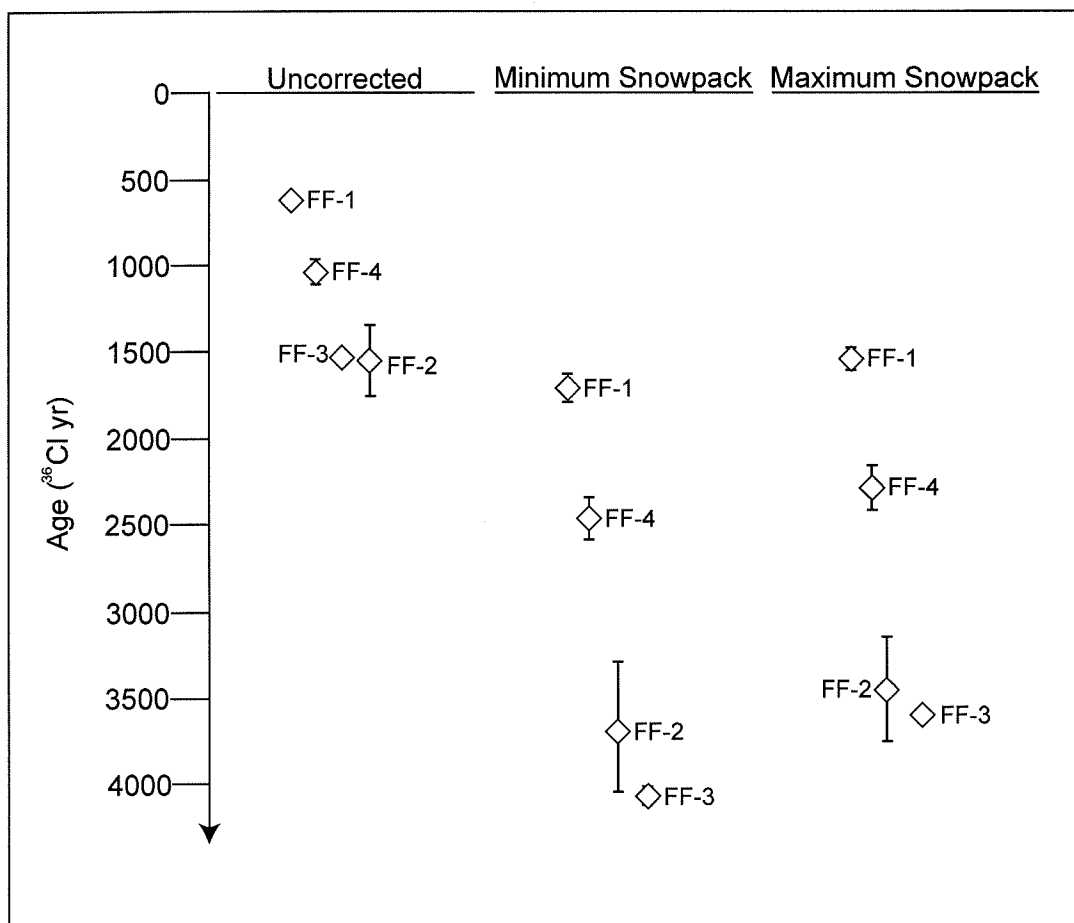


Figure 13: Graph of Williwakas Glacier/Fairy Falls surface-exposure ages. Graph of uncorrected and snowpack-corrected surface-exposure ages with 1-sigma error bars (error encompassed by symbol when not shown) for the Williwakas Glacier/Fairy Falls site samples.

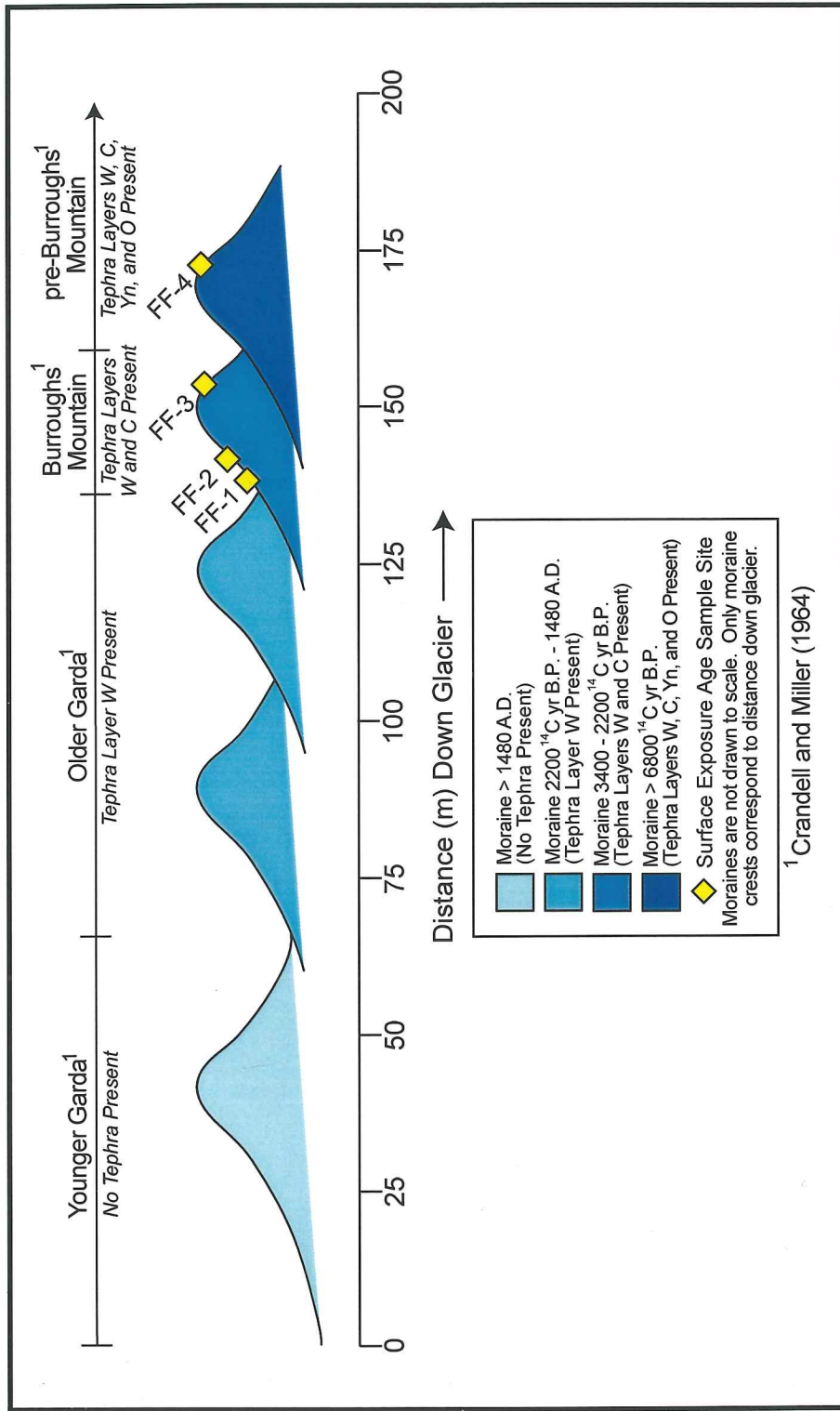


Figure 14: Profile of the Williwakas Glacier/Fairy Falls moraines with surface-exposure ages and sample locations. Diagrammatic profile across Williwakas moraines, showing tephrochronologic limiting ages and surface-exposure sample locations.

Sample FF-4 comes from a boulder on the distal side of the outermost moraine that has a minimum limiting tephrochronologic age of 7650 cal yr BP. Sample FF-3 is from a boulder lying on the proximal side of the next younger moraine. The uncorrected boulder ages are both younger than age of tephra layers Yn and C. A possible reason for the anomalously young ^{36}Cl age of FF-4 is that the boulder moved off the crest of the moraine long after deposition, exposing a fresh surface to cosmic radiation. Another possibility is related to the closeness of these moraine segments, meaning that ice of the younger advance may have deposited boulders on top of the moraine of an older advance (i.e., the outer moraine was overridden and is cored by older drift). The outermost moraine's tephrochronologic age of >7650 cal yr BP makes a late-glacial or mid-Holocene age possible. Tephra layer O lies at ca. 10 cm depth adjacent to the boulder, whereas the sampled boulder lies *on* the surface of the moraine making possible its deposition after tephra layer O and after moraine deposition. If the sampled boulders were exhumed and found *at* the surface of the moraine they would belong to that moraine and therefore must be older than tephra layer O (7650 cal yr BP)(Fig. 4).

Sample FF-2 lies on the proximal side of a moraine with limiting tephrochronologic ages of 3650 and 2225 cal yr BP. The snowpack-calibrated age range of FF-2 is 3470-3700 ^{36}Cl yr BP, consistent with the tephrochronology, and implies correlation with Crandell's (1969) Burroughs Mountain Drift (3650-2225 cal yr BP).

Sample FF-1 also is from the proximal side of the second moraine segment. However, sample FF-1 has a snowpack-calibrated age of 1700-1550 ^{36}Cl yr BP. This age is at least 480 yr younger than the minimum limiting tephrochronologic age of 2225 cal yr BP. Possibly, the boulder was displaced (rolled) after deposition, was exhumed, or had a different snowpack history than the FF-2 boulder. The crest of the nearest Older Garda moraine has an age of 2200 ^{14}C yr BP - 1480 A.D. based on tephrochronology. This Neoglacial moraine is more than 30 m from the second (FF-1, FF-2) moraine, thereby eliminating the possibility that these boulders rolled off that younger moraine.

The third and fourth moraine segments are overlain by tephra layer W (Fig. 12). These moraines lack boulders suitable for ^{36}Cl dating, but likely correlate with Crandell's (1969) Older Garda (early LIA) deposits. The fifth moraine segment lacks tephra and must be less than 524 yr old; it corresponds to Crandell's (1969) Younger Garda (late LIA) deposits.

Figure 15 shows a profile of Williwakas Glacier at the time the Fairy Falls moraines were built. Ice thickness in the lower part of the glacier is based on the mapping of partially eroded lateral moraines and glacially eroded bedrock found on the ridge just northeast of the Fairy Falls site. The extent of Williwakas Glacier during its maximum Holocene extent is shown in Figure 11, along with surface contours and ELAs (Sec. 4).

3.4 BERKELEY PARK SITE

One distinct moraine has been mapped in the north-facing Berkeley Park basin (Fig 16). The moraine outlines the former terminus of a small ($<2\text{ km}^2$) glacier that descended from the ridge separating Berkeley Park and the Granite Creek basin to the west. The moraine is overlain by tephra units O and R. Therefore, the age of the moraine must be $>10,025\text{ cal yr BP}$ ($8850\text{ }^{14}\text{C yr BP}$), the age of layer R.

Six surface-exposure age samples were taken from boulders $>0.75\text{ m}$ in diameter from the crest of the Berkeley Park moraine (Figs. 16, 17, 18; Table 9). All the sampled boulders lay close to the crest of the moraine on its proximal slope.

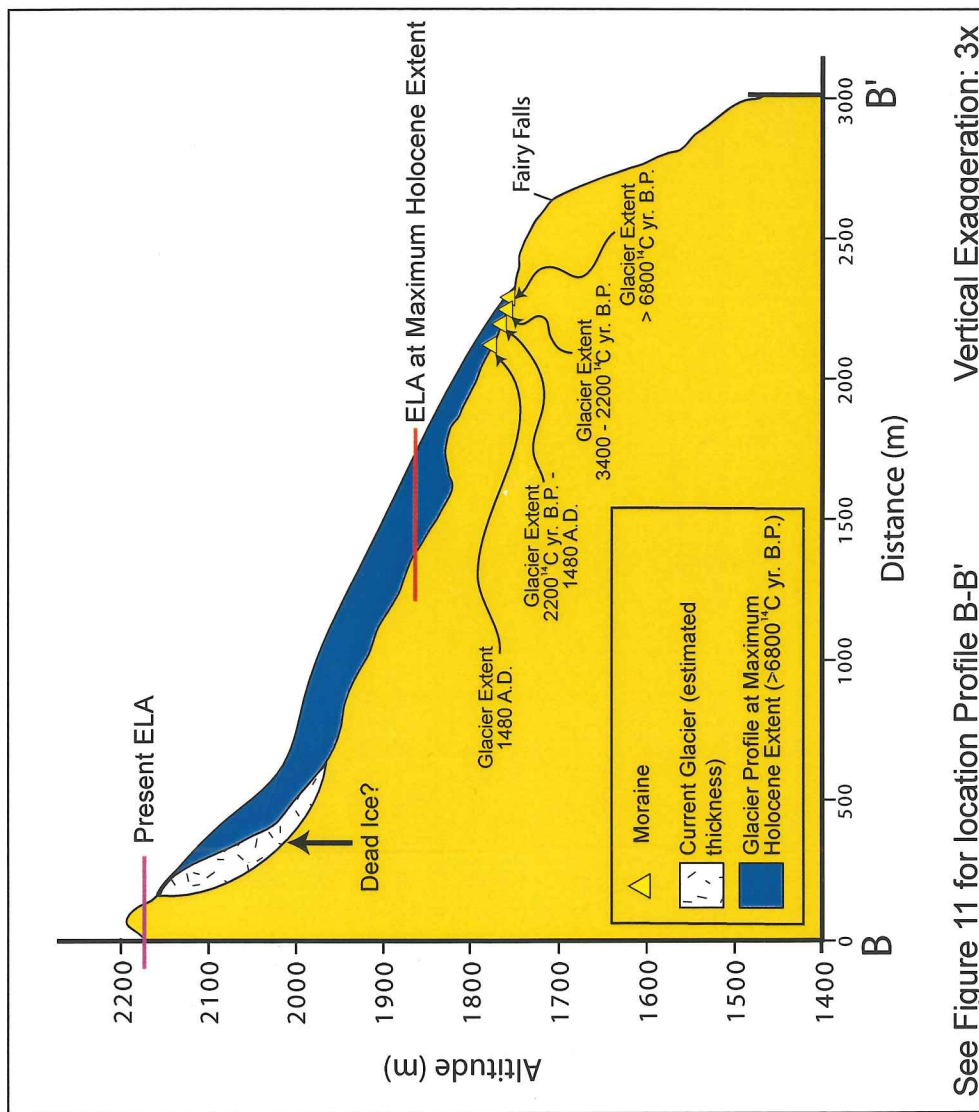


Figure 15: Profile of glacier that deposited the Williwakas Glacier/Fairy Falls moraines. Williwakas Glacier, showing paleo-ELA, at the time when the outermost moraine at the Fairy Falls site was deposited.

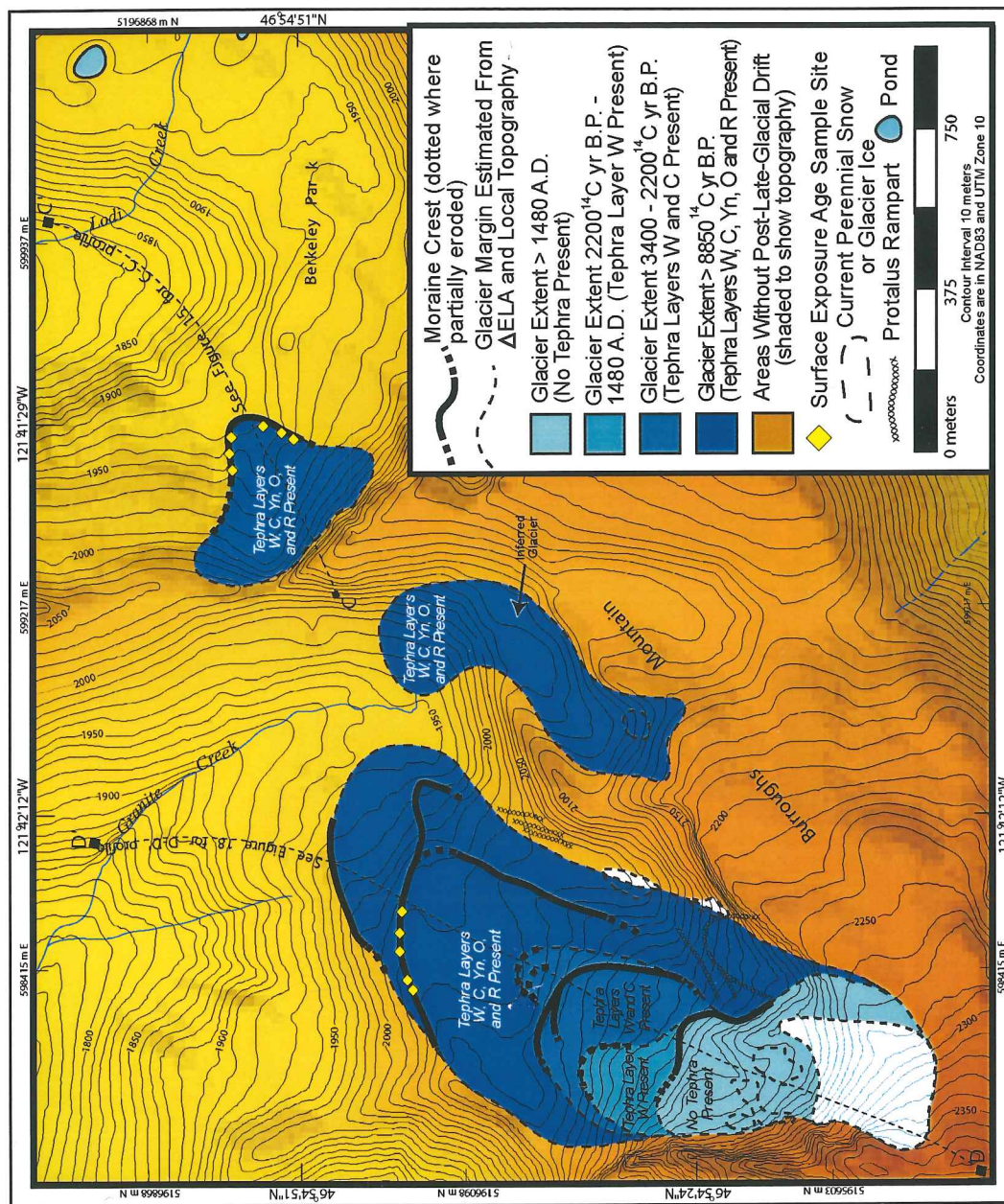


Figure 16: Map of the Berkeley Park and Granite Creek field sites. The sites are on Burroughs Mountain showing moraines, former glacier extent, tephra units, and surface-exposure sample localities.

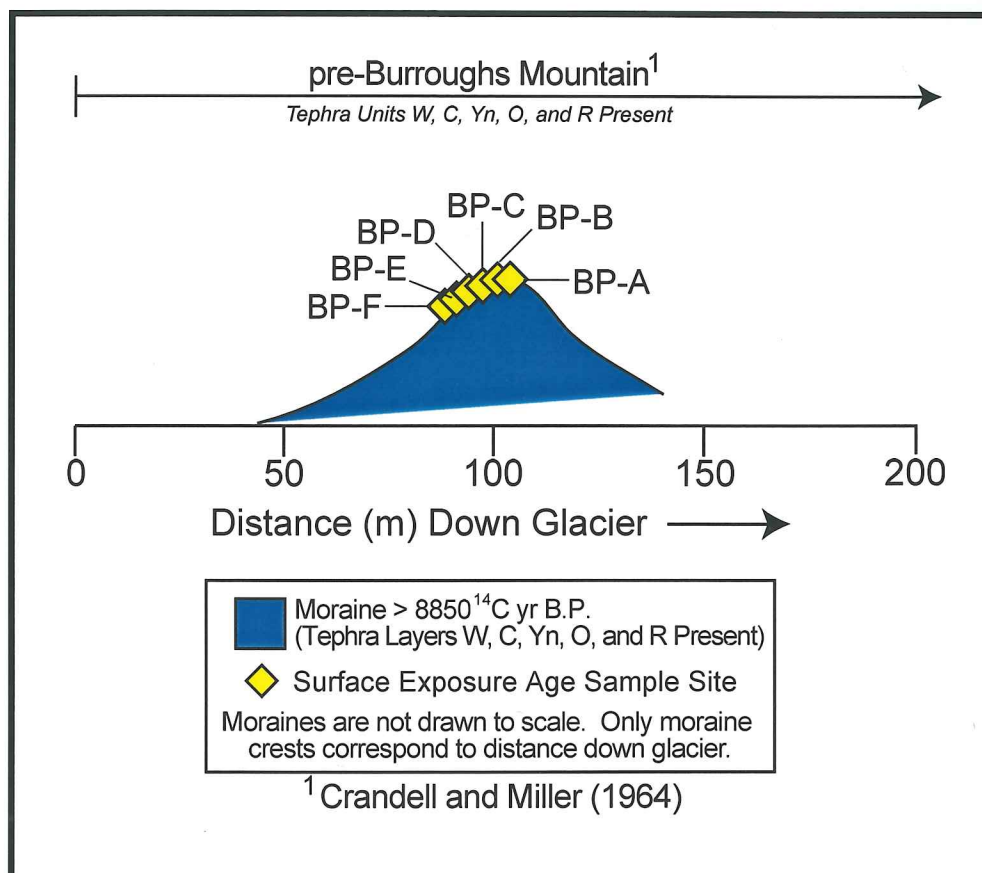


Figure 17: Profile of the Berkeley Park moraine with surface-exposure age sample locations. Diagrammatic cross-section of the moraine at the Berkeley Park site with its tephrochronologic limiting ages and surface-exposure sample locations.

**Table 9: ^{36}Cl Surface-exposure Ages¹
for the Berkeley Park field site**

Sample	Uncorrected Age ² (^{36}Cl yr)	Minimum Snowpack ³ Depth Age (^{36}Cl yr)	Maximum Snowpack ³ Depth Age (^{36}Cl yr)	Tephro- chronologic Age of Moraine at Sample Site (^{14}C yr)
BP-A	12,280 ± 760	27,020 ± 1680	21,190 ± 1320	>8850
BP-B	10,690 ± 670	21,860 ± 1380	17,400 ± 1100	>8850
BP-C	13,390 ± 840	30,940 ± 1950	24,000 ± 1510	>8850
BP-D	9490 ± 220	19,300 ± 450	15,320 ± 360	>8850
BP-E	7670 ± 40	15,610 ± 80	12,440 ± 60	>8850
BP-F	10,040 ± 650	20,270 ± 1310	15,870 ± 1030	>8850

¹The ages reported are based on an assumption of no erosion and include 1σ error.

²Rounded to the nearest decade.

³The snowpack has a mean annual density of 0.5 (Ebbesmeyer and Strickland, 1995). An explanation of this value is given in Section 2.4.

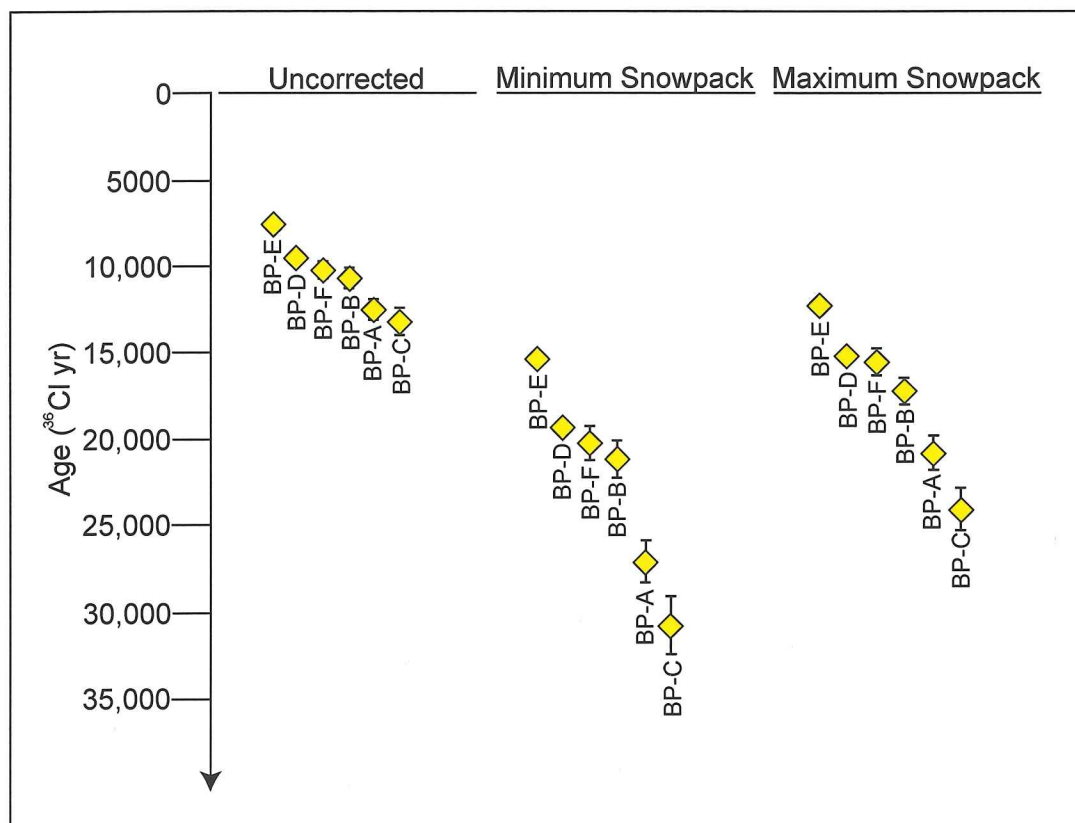


Figure 18: Graph of Berkeley Park surface-exposure ages. Showing uncorrected and snowpack-corrected surface-exposure ages with 1-sigma error bars (error encompassed by symbol when not shown) for the boulder samples.

The tephrochronologic minimum limiting age of the Berkeley Park moraine is 10,025 cal yr BP (>8850 ^{14}C yr BP) because layer R is found on it. Except for the highest adjacent ridges, Berkeley Park was covered by glacier ice during the LGM (Crandell, 1969). Reduced snowpack values are used in calculating ages of samples taken on the northeastern side of Mount Rainier due to the precipitation shadow effect. The scattering of the uncorrected ^{36}Cl ages suggests moraine or boulder degradation which is supported by the site being above tree line. The snowpack-calibrated ages for 4 of the 6 samples taken are consistent with an LGM age. Taken alone, the minimum snowpack-calibrated ages of samples BP-A and BP-C are too old to be valid if LGM ice overrode this area. The mean age of the moraine with the maximum estimated snowpack is 17,700 ^{36}Cl yr BP, which is close to the time of maximum advance of the Puget Lobe (Porter and Swanson, 1998). If a prior exposure history for boulders BP-A and BP-C is inferred, the minimum snowpack ages in Table 10 might be reasonable. The mean uncorrected age of the moraine is $\sim 10,600$ ^{36}Cl yr BP, a reasonable minimum date for a Younger Dryas-age advance. However, this would be the only Younger Dryas-age moraine yet found on Mount Rainier, and, this age also fits Heine's (1997) McNeely 2 (early Holocene) advance. The moraine was likely deposited during the late Pleistocene and may mark the LGM (i.e., ca. 22,000-17,000 cal yr BP). The moraine lies above a large glacial trough (Plate 1, Fig. 16) that was likely filled with ice during the LGM, making a late-glacial age for the moraine more reasonable.

Figure 19 illustrates the profile of the glacier, based on Figures 16 and 20, responsible for the Berkeley Park moraine. The full extent of the Berkeley Park Glacier at the time the moraine was deposited is shown with glacier surface contours and ELA (see Section 4) in Figure 20.

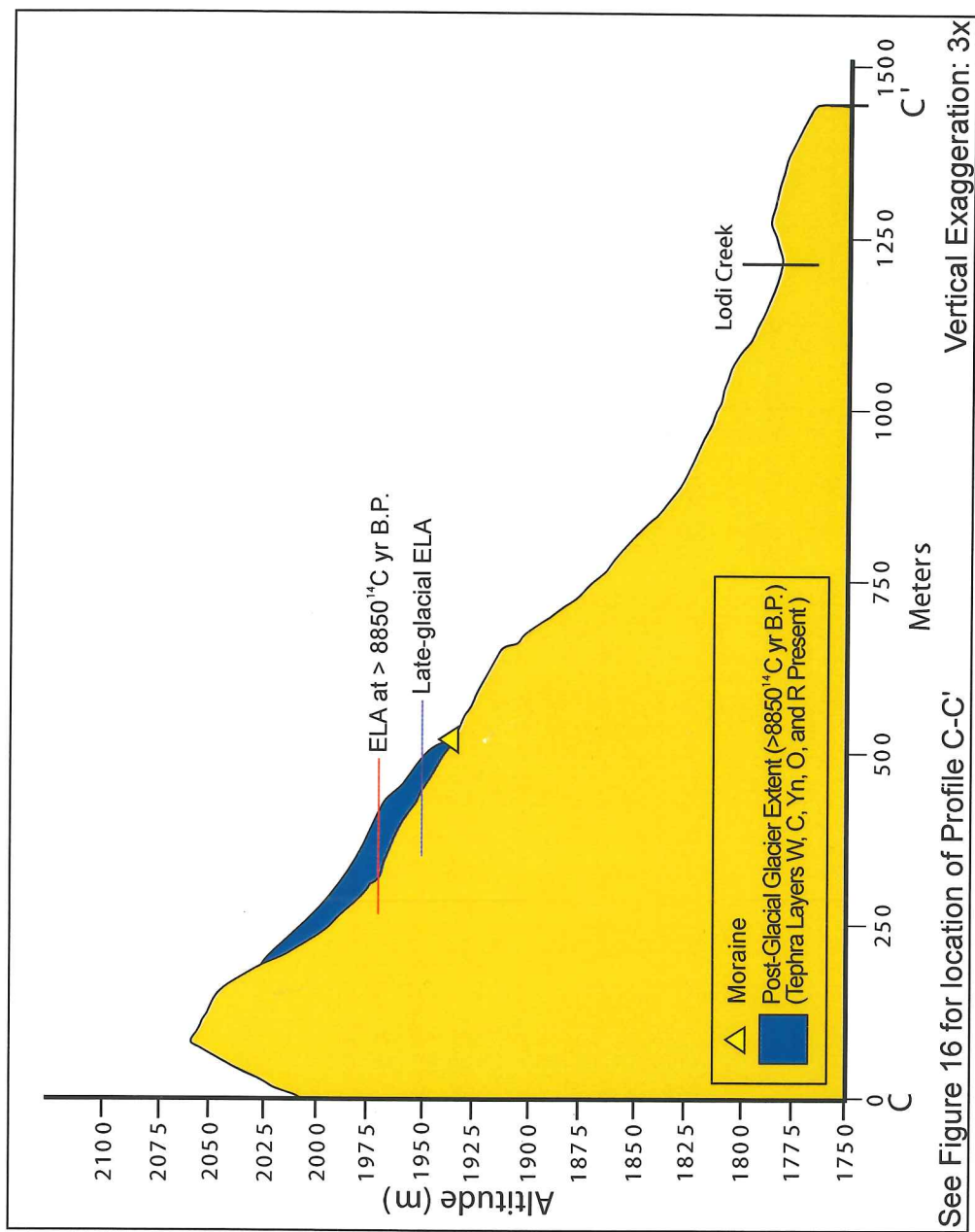


Figure 19: Profile of the glacier that deposited the Berkeley Park moraine. Showing paleo-ELA, at the time when the moraine was deposited.

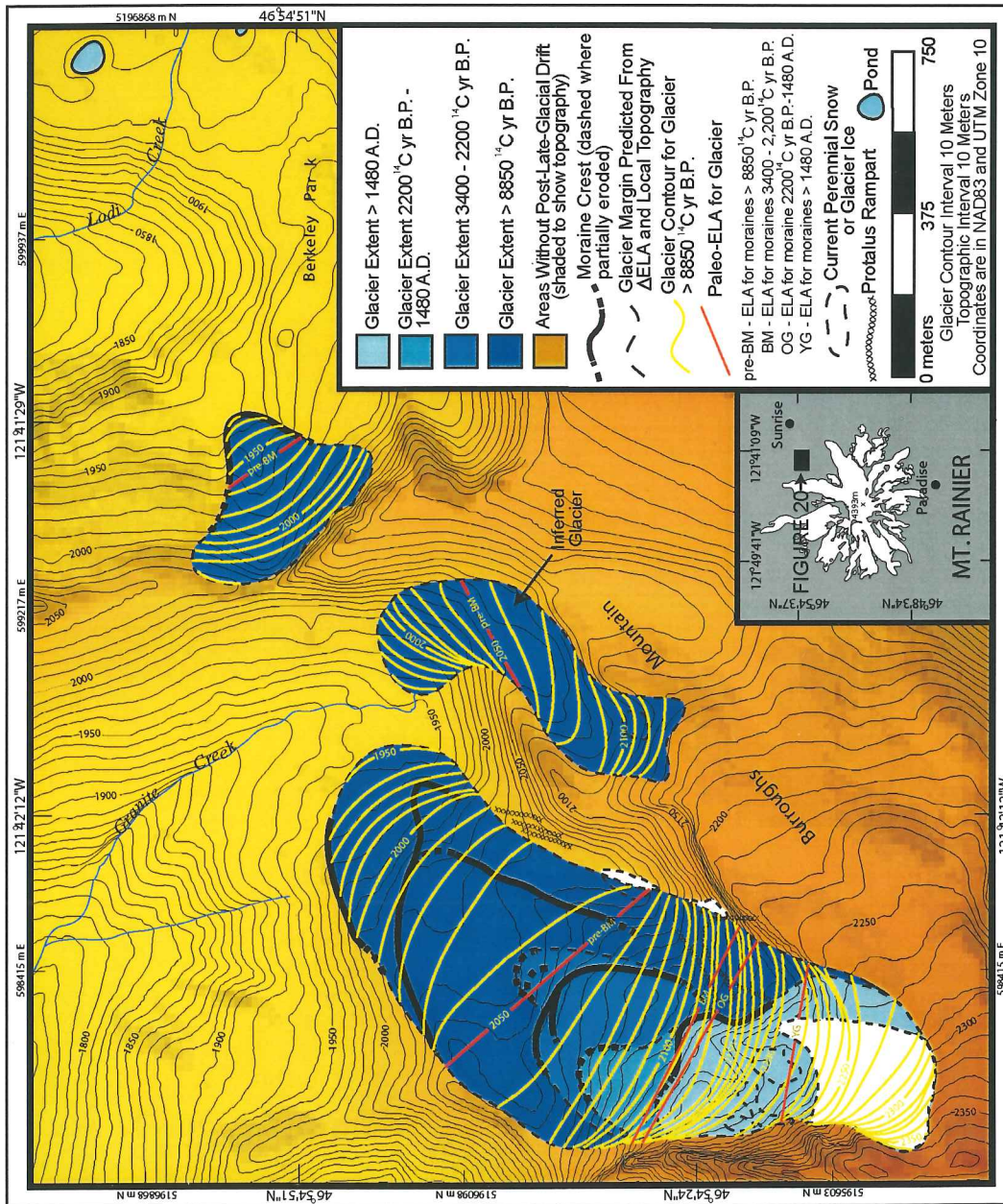


Figure 20: Granite Creek and Berkeley Park glacier surface altitude map. Map showing the extent of the glaciers responsible for the Berkeley Park and Granite Creek moraines, with glacier contours (m), during deposition of the youngest pre-Burroughs Mountain drift.

3.5 GRANITE CREEK SITE

Nine moraine segments were mapped in the Granite Creek basin below Burroughs Mountain (Fig. 16). The lowest three segments are covered by tephra units Yn, O and R giving these segments a minimum limiting age of 8850 cal yr BP. These are the only moraines in the Granite Creek basin with boulders capable of being sampled for surface-exposure dating. Four moraine segments are covered by tephra layers W and C, but not unit Yn, placing their age of between 3650 and 2225 cal yr BP corresponding with Crandell's (1969) Burroughs Mountain drift. One segment is overlain by layer W but not layer C giving it bracketing ages of 2200 ^{14}C yr BP and 1480 A.D. (Older Garda Drift). One of the youngest two moraine segments mapped lies on the small bedrock ridge that bounds the northwest side of the Granite Creek basin. This deposit dates to the late LIA, for it lacks tephra layer W and is a lateral moraine of Winthrop Glacier. The other moraine segment is the highest segment in the Granite Creek basin. The segment encloses the bottom of a small cirque in which perennial snowpatches are now found. This segment also lacks tephra layer W and therefore, is <524 yr old.

Five samples for surface-exposure dating were taken from boulders >1 m in diameter from the crest of the innermost of the oldest moraine segments in Granite Creek basin (Figs. 16 and 21). The snowpack-calibrated ages of the samples are shown in Table 10 and Figure 22.

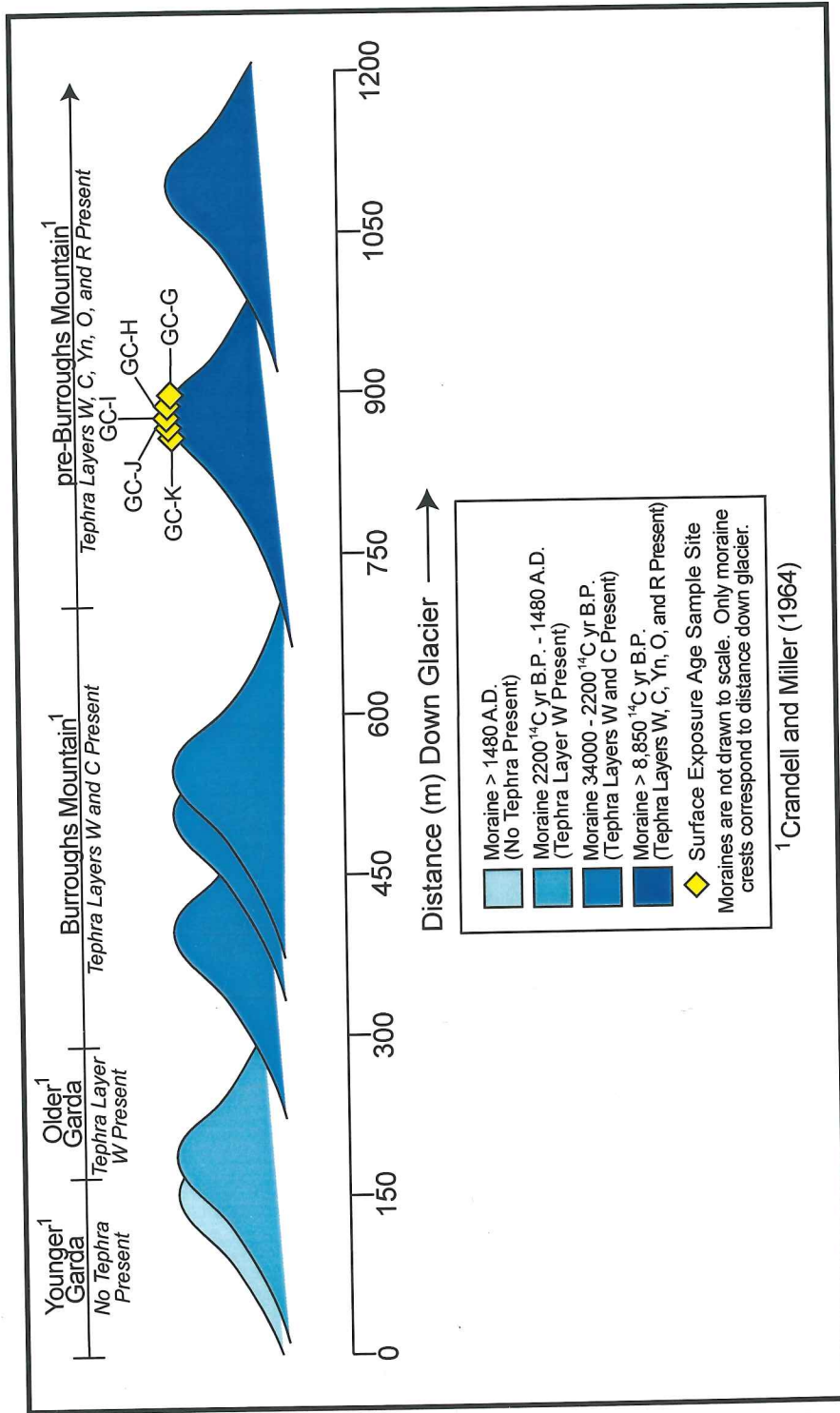


Figure 21: Profile of the Granite Creek moraines with surface-exposure age sample locations. Diagrammatic profile of the moraines with their tephrochronologic limiting ages and surface-exposure sample locations.

**Table 10: ^{36}Cl Surface-exposure Ages¹
for the Granite Creek field site**

Sample	Uncorrected Age ² (^{36}Cl yr)	Minimum Snowpack ³ Depth Age (^{36}Cl yr)	Maximum Snowpack ³ Depth Age (^{36}Cl yr)	Tephro- chronologic Age of Moraine at Sample Site (^{14}C yr)
GC-G	10,610 ± 820	22,120 ± 1720	17,610 ± 1370	>3400
GC-H	8950 ± 10	19,920 ± 20	15,650 ± 10	>3400
GC-I	34,430 ± 940	79,990 ± 2180	60,740 ± 1660	Outlier (reworked)
GC-J	3900 ± 140	8470 ± 300	6660 ± 240	Outlier (exhumed or displaced)
GC-K	15,820 ± 350	26,090 ± 580	23,290 ± 510	>3400

¹The ages reported are based on an assumption of no erosion and include 1σ error.

²Rounded to the nearest decade.

³The snowpack has a mean annual density of 0.5 (Ebbesmeyer and Strickland, 1995). An explanation of this value is given in Section 2.4.

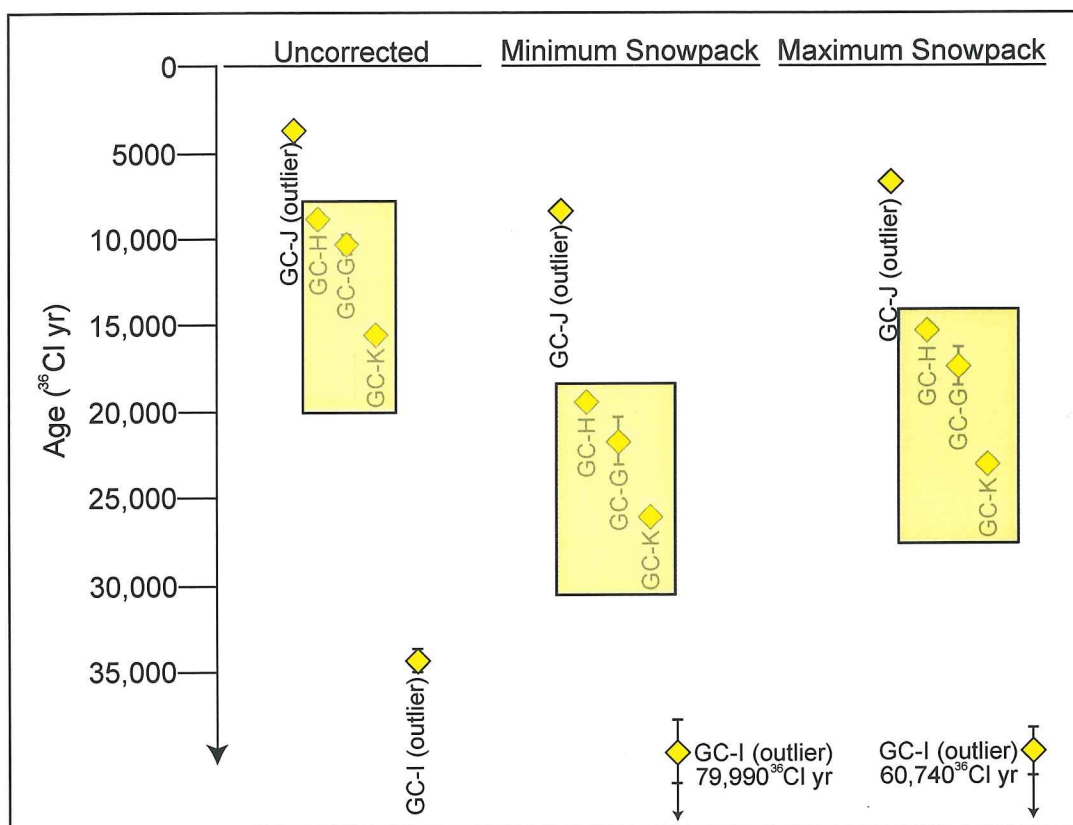


Figure 22: Graph of Granite Creek surface-exposure ages. Showing uncorrected and snowpack-corrected surface-exposure ages with 1-sigma error bars (error encompassed by symbol when not shown) for the boulder samples.

The five analyzed samples range widely in age. The uncorrected and snowpack-calibrated surface-exposure ages of samples GC-G and GC-K agree with their stratigraphic position below tephra layer R (10,025 cal yr BP). Sample GC-H has a ^{36}Cl age slightly younger than the presence of tephra layer R below the sampled boulder suggests. GC-I is an obvious outlier, with an uncorrected surface-exposure age of 34,430 ^{36}Cl yr, and likely is reworked from older drift [i.e., prior exposure (pre-LGM)]. Sample GC-J, with an uncorrected age of 3900 ^{36}Cl yr BP, came from a boulder that apparently moved after deposition or was exhumed. The seemingly reliable uncorrected ^{36}Cl ages of samples GC-G and GC-K, along with the tephrochronologic age of the moraine segment, suggest it may represent a late-glacial recessional moraine or a readvance.

The limit of glacier ice in a small cirque between Burroughs Mountain and Berkeley Park moraine (Figs. 16 and 20) is not based on sedimentary evidence but rather on the reconstructed late-glacial ELA. It is likely that this small cirque glacier was confluent with the larger glacier in the Granite Creek cirque during the early LGM recessional phase.

Figure 23 illustrates the long profile of the glacier that built the mapped moraines in the Granite Creek basin based on data from Figures 16 and 20. The full extent of the Granite Creek Glacier during the times of moraine deposition is shown in Figure 20, along with surface contours and ELAs (Sec. 4).

3.6 TALUS AND COLLUVIAL FAN STRATIGRAPHY AND CHRONOLOGY

Sliderock is produced by mechanical weathering of bedrock associated with freezing and thawing of water in cracks and pore spaces. A talus forms beneath a cliff that has undergone numerous freeze-thaw cycles. Stable taluses are datable on Mount Rainier using tephra stratigraphy in the same manner as glacial deposits.

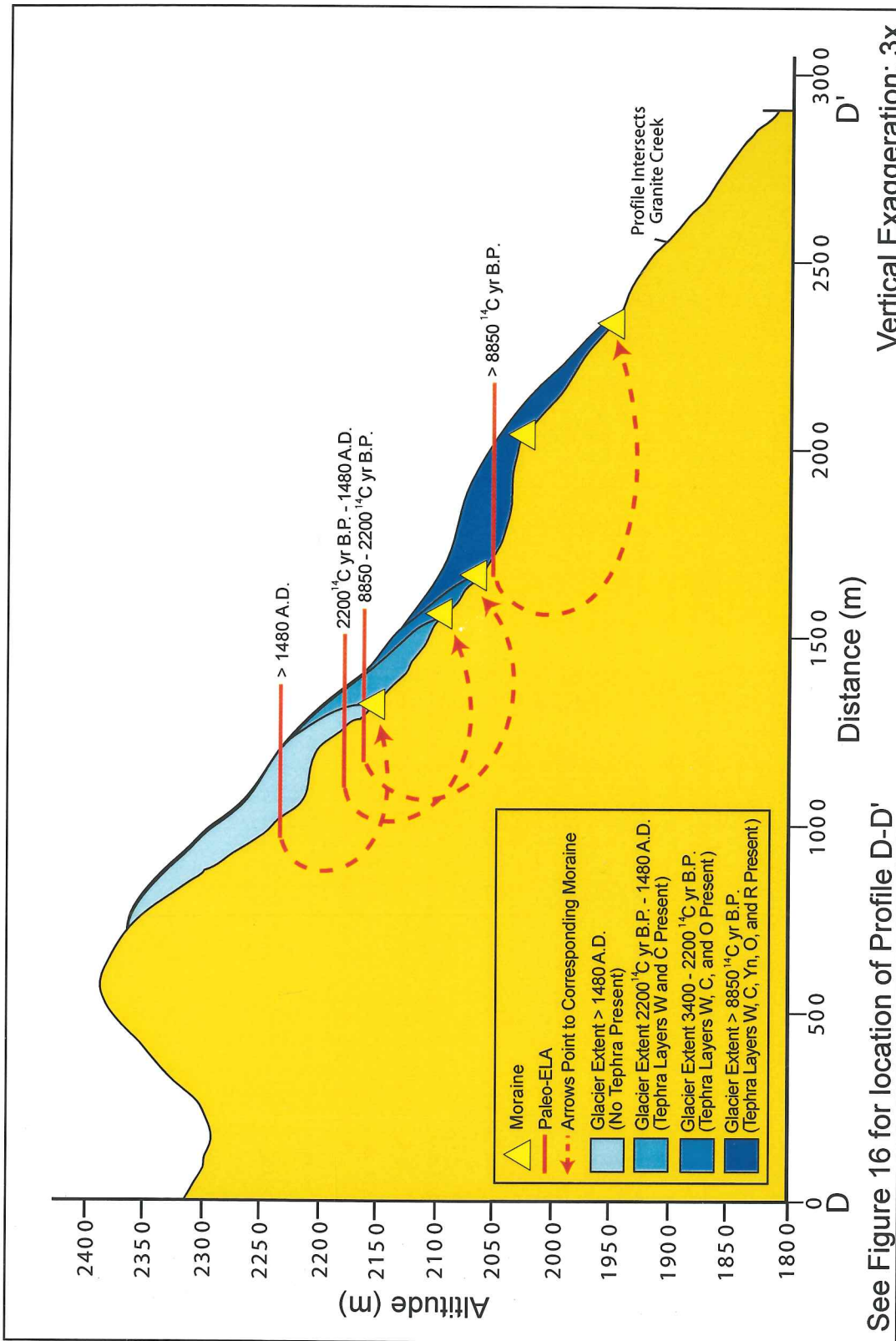


Figure 23: Profile of the glacier that deposited the Granite Creek moraines. Showing altitudes, corresponding tephrochronologic limiting ages and paleo-ELAs of inferred from the moraines.

If climate deteriorates at Mount Rainier, a cliff may be subject to an increased frequency of freeze-thaw cycles and a reduction in stabilizing vegetation cover, and will produce more frost-derived sediment than during warmer periods. The volume of taluses in glaciated basins therefore may increase during a cool climatic episode.

Sliderock in a talus 150 m below the Paradise field site along the Sluiskin Falls trail (Fig. 11) is interbedded with tephra layers (Figure 24). The talus beneath the rocky outcrop forms three overlapping lobes that are younger from east to west. The slope is underlain by polished and striated quartz monzonite of the Tatoosh Pluton, recently exposed where a stream has eroded overlying sediment. The quartz monzonite is overlain by a bouldery till, likely of late-glacial age. Tephra layer O rests on the till. The absence of soil or colluvium between the till and tephra layer O suggests that the till is close in age to the age of layer O (7650 cal yr BP) or that slope erosion occurred prior to deposition of layer O. The tephra is overlain by oxidized, clay-rich sediment of the Paradise Lahar. Above the lahar deposit are other, less-easily identifiable Rainier tephras that are interbedded with brownish, fine to medium-grained colluvium. The oldest talus lobe overlies ~8 cm of tephra layer Yn (3650 cal yr BP), which is a maximum limiting age for the lobe. A minimum limiting age of the oldest lobe comes from tephra unit C (2225 cal yr BP), which lies at or near the base of second talus lobe and overlies the older lobe. The limiting ages of 2225 and 3650 cal yr BP for the oldest lobe imply correlation with Burroughs Mountain Drift. Tephra unit W (1480 A.D.) directly overlies the talus lobe that lies above tephra unit C. With limiting age between 2200 ¹⁴C yr BP and 1480 A.D., the second talus lobe may correspond to the Older Garda Drift. The youngest lobe postdates layer W and formed during the late LIA. The boulders making up this lobe have fresh, angular surfaces with minimal ($\leq 5\%$) lichen cover and *Rhizocarpon geographicum* thalli diameters of < 2 cm. Porter's (1981b) lichen growth curves for *Rhizocarpon geographicum* on the granodiorite and andesite of Mount Rainier shows that these lichens are no older than ca. 40 yr. Boulders incorporated in the older lobes lack lichens that would yield reliable ages because they are covered by colluvium.

Age (cal yr BP)	Unit	Graphic Section	Description
470	Qt		Talus deposit: angular boulders <50 cm diameter, clast supported, minimal lichen cover, no soil or matrix developed
	W		White, sand-sized ash, at or near surface
	Qs		Poorly developed soil with organics
2225	Qt		Talus deposit: angular boulders <30 cm diameter, clast supported with fine to medium sand matrix
	C		Brown lapilli deposit at or near surface
	Qs		Moderately developed soil with organics
3650	Qt		Talus deposit: angular to sub-angular boulders <30 cm diameter, clast and matrix supported, fine sand matrix
	Yn		Yellow, coarse ash with sparse black lithics
	Qmf		Paradise Lahar, clay-rich, partially oxidized with clast up to 30 cm with unidentified Rainier tephra
7650	O		Reddish-yellow to pale yellow light colored ash
	Qm		Late-glacial till, either McNeeley 1 or 2 <i>unconformity</i>
	Tg		Quartz monzonite of the Tatoosh Pluton, 17.5-14.1 million years old

Figure 24: Idealized chronostratigraphic section of talus near the Paradise Glacier site (not to scale). Including tephra layers, lahar sediment, and till interbedded with the sliderock of the talus.

4. SYNTHESIS

4.1 RESPONSE OF GLACIERS TO CLIMATIC AND TOPOGRAPHIC INFLUENCES

Temperature shifts are not always coincident with shifts in precipitation. A glacier may experience a change in mass balance with a shift in temperature or precipitation, or both. From the glacial-geologic record alone, one cannot determine if a moraine was formed due to a change in precipitation or a change in temperature or both. A sustained increase in precipitation will generally have a positive affect on the mass balance of a glacier, given no change in mean annual temperature. Likewise, a reduction in mean annual temperature, especially summer temperature, could lead to reduced ablation, also producing a positive mass balance.

The lag time between a change in mass balance due to a climatic change and an advance of the terminus (response lag) varies according to the length, slope, and temperature of the glacier. An average lag time between an increase in precipitation and an advance of the terminus of small (<10 km²) temperate alpine glaciers, such as those on Mount Rainier, is ca. 10 to 100 years (Johannesson et al., 1989) because of steep alpine slopes, well-lubricated beds, and rapid mass turnover (i.e., high activity).

Local topography also affects the response lag. Gravity will force a glacier flowing down a steep gradient to flow faster than a glacier flowing over the same bed but with a lower gradient. The faster flow is able to transfer mass from above the ELA to the terminus more rapidly than if the glacier was flowing slowly over a gentle gradient. On Mount Rainier this may cause the relative disposition of terminal moraines to vary from site to site, for valley slopes vary widely around the mountain.

Terminal positions also vary spatially on Mount Rainier because of the local precipitation shadow produced by the mountain. On average, most winter storms reach Mount Rainier from the southwest². This leads to higher precipitation for the sites on the southern and

² From the Mount Rainier National Park website: <http://www.nps.gov/mora/current/weather.htm#cause>.

western sides of the mountain than on the northeastern side. Glaciers on open slopes on the northeastern side of the mountain would receive less direct insolation each day than those on the southwestern side, thereby reducing loss of snow and ice by ablation.

4.2 LATE PLEISTOCENE AND HOLOCENE EQUILIBRIUM LINE ALTITUDES

The precipitation shadow and mean temperature difference across the mountain leads to a rise in ELAs from the southwestern side to the northeastern side of the mountain. Both Heine (1997) and Nylén (1998) reconstructed glaciers on or near Mount Rainier based on moraine positions, mapped in the field and interpreted from aerial photographs, and glacier headwall positions. The ELA was reconstructed using the accumulation-area ratio method (AAR) with a ratio of ca. 65:35 for the accumulation area:ablation area (Porter, 1975, 2001). The average ELA of glaciers on the southwestern side of the mountain is 2200 m, whereas the average of those on the northeastern side is 2400 m (Heine, 1997; Nylén, 1998).

The regional ELA depression in the southern North Cascade Range at the last glacial maximum was ca. 900 m (Porter et al., 1983). This ELA depression is consistent with the ca. 920 m LGM depression for Nisqually Glacier at the LGM reported by Heine (1997). There are no published data for an LGM ELA on the northern or northeastern sides of Mount Rainier.

Heine (1997) reports a late-glacial (McNeely 1) ELA depression of ca. 450 m for cirque glaciers to the east and northeast of Mount Rainier but there are no data on the late-glacial ELA depression on the southern side of the mountain. Lacking reliable ELA gradients across the mountain for the LGM and late-glacial advances, I assume that the current ELA gradient (ca. 25 m/km) (Nylén, 1998) across the mountain has been constant during the late Quaternary (Porter, 2001). This places the LGM ELA on the southwestern and northeastern sides at 1300 and 1500 m, respectively. Using the same assumptions, the

late-glacial ELA on the southwestern side would have been at ca. 1750 m and on the northeastern side at ca. 1950 m.

ELAs corresponding to the mapped moraines at each field site were determined using the AAR method (Porter, 1975). Glacier margins were inferred and mapped using the positions of the glacier headwall and moraines (Figs. 11 and 20).

4.2.1 PARADISE GLACIER EQUILIBRIUM LINE ALTITUDES

The modern ELA of Paradise Glacier is 2175 m (Nylen, 1998) (Figs. 10 and 11). The ELA determined from the outermost moraine in the basin containing the Paradise moraines is ca. 1980 m (Figs. 10 and 11). The late-glacial ELA, representing a 450 m depression, would have been at 1720 m, about 160 m lower than the altitude of the most distal Paradise moraine (Fig. 7). The bedrock surface of sample PG-2 (Fig. 7) likely would have been covered by glacier ice during the late-glacial/early Holocene advances (McNeely 1 and 2). The low ELA of McNeely-age glaciers, the age of the bedrock surface (PG-2), and the presence of tephra layer O at the site indicate that ice last overflowed the basin containing the Paradise moraines more than 7650 cal yr BP (6800 ^{14}C yr BP) ago. The corrected ^{36}Cl age of the moraine is similar to the calibrated ^{14}C age of the McNeely 1 moraines, which represent an ELA depression of ca. 450 m.

The tephra stratigraphy on the moraines suggests that the outer Paradise Glacier moraine segment could be correlative with Heine's (1997) McNeely 1 or 2 advances; however, the lower, late-glacial ELA likely represents a late-glacial recessional stand or readvance. The ELA equivalent to the younger moraines of Paradise Glacier at this site would have been only slightly higher (ca. 20-30 m) than the ELA of the glacier that deposited the outermost moraines. Therefore, the late-glacial and earliest Neoglacial moraines must have had comparable mass balances and ELAs. This implies that the former must postdate the McNeely 2 maximum.

4.2.2 WILLIWAKAS GLACIER EQUILIBRIUM LINE ALTITUDES

Nylen (1998) placed the modern ELA of Williwakas Glacier at 2050 m (Figs. 10 and 11). This is 125 m lower than the modern ELA of adjacent Paradise Glacier. It seems more likely that the modern ELA of Williwakas Glacier is closer to that of the adjacent Paradise Glacier (ca. 2175 m). This would place the modern ELA at a greater elevation than any part of Williwakas Glacier, suggesting that the glacier is slowly ablating stagnant ice instead. The ELA corresponding to the outermost moraine of the Williwakas Glacier site is ca. 1980 m, the same as Paradise Glacier's ELA at this time (Figs. 10, 11, 15). The late-glacial ELA for Williwakas Glacier would have been ca. 1720 m. This is the approximate elevation of the most distal moraine at the Fairy Falls site. As at the Paradise Glacier site, the tephra stratigraphy indicates that the outermost moraine could have a late-glacial age; however, when the paleo-ELA is considered, the moraine more likely is a late-glacial recessional moraine. The ELA of Williwakas Glacier represented by the nested younger moraines would have been only slightly higher (ca. 20-30 m) than the ELA of the glacier responsible for the outermost moraines. This argues against it being a McNeely 2 equivalent moraine.

4.2.3 BERKELEY PARK GLACIER EQUILIBRIUM LINE ALTITUDES

On the north side of the mountain, the late-glacial ELA was at ca. 1975 m (Heine, 1997). This is approximately the same altitude as the reconstructed ELA for the Berkeley Park moraine. The >8850 ^{14}C yr BP tephrochronologic age of the Berkeley Park moraine and the 1965 m ELA (Figs. 19 and 20) approximate the age and ELA of Heine's (1997) McNeely advances. The tephrochronology and the mean *uncorrected* ^{36}Cl age of the moraine support the oldest moraine at the Berkeley Park site being late-glacial in age. However, the mean *corrected* ^{36}Cl age of the Berkeley Park moraine indicates an LGM-age which is not possible if LGM glacier ice completely covered the Berkeley Park area (Crandell, 1969).

4.2.4 GRANITE CREEK GLACIER EQUILIBRIUM LINE ALTITUDES

The multiple moraines at the Granite Creek site are farther apart than the moraines at the Paradise and Fairy Falls sites. Upper glacier limits are defined better, and so the individual ELAs for each ice advance can be estimated closely (Figs. 20 and 23). The ELA corresponding to the outermost moraine would have been ca. 2050 m. The ELA for the Burroughs Mountain advance would have been ca. 2160 m, the Older Garda ELA was ca. 2180 m, and the ELA of the Younger Garda glacier would have been ca. 2230 m. The Δ ELA from the outermost moraine (pre-Burroughs Mountain) to the innermost moraine (Younger Garda) is 180 m. For the Granite Creek moraines, the late-glacial ELA was at the same altitude as the outermost mapped Holocene moraine suggesting that if this moraine was late-glacial in age it likely is a recessional moraine. There are no late-glacial moraines lower in the Granite Creek valley that would allow the late-glacial ELA to be closer to 1975 m, which is the ELA inferred from the Berkeley Park moraine ca. 1 km to the east of the Granite Creek moraines. If the ELAs on the southeast and northeast sides of Mount Rainier are compared, an ELA gradient similar to the late Pleistocene ELA gradient and the present gradient of ca. 25 m/km (Heine, 1997 and Nylén, 1998) apparently existed throughout the latest Pleistocene and Holocene.

The 1997 ELA lies at 2400 m on the north side of Mount Rainier based on late summer ELAs mapped from aerial photographs (Heine, 1997 and Nylén, 1998). The crest of Burroughs Mountain, which lies at the head of the cirque containing the Granite Creek moraines, is 2386 m. Crandell (1969) mapped a small, unnamed glacier at the head of the cirque, just inside the Younger Garda Moraine (Fig. 16). It is questionable whether this is a dying glacier (there currently is no active moraine formation) or perennial snow. If it is a glacier with a balanced regime it would lower the modern ELA on the north side of the mountain by ca. 50 m.

Based on the tephrochronology, consistent surface-exposure ages (not including the outliers GC-I and GC-J), and proximity, the outermost Granite Creek moraine and the

Berkeley Park moraines likely represent a coeval ice advance. However, there is an 85 m difference in the corresponding ELAs of these moraines. The ELA of the Berkeley Park moraine should be slightly higher than the Granite Creek ELA because the Granite Creek glacier would have had a north-facing aspect and Berkeley Park glacier would have had an east-facing aspect, exposing it to more solar radiation and ablation. Because of this ELA difference, the Berkeley Park moraine may actually be a protalus rampart. The different lithologies and glacial striations on the boulders at the Berkeley Park site could be explained by a reworking of older glacial drift into the protalus rampart from the ridge above the site.

4.3 COMPARISON WITH PREVIOUS RESEARCH

The evidence for climatic shifts during Neoglaciation is widespread on Mount Rainier. However, correlation with other paleoclimate proxies from the rest of the world is difficult because of the wide constraints of tephrochronologic limiting dates for each advance on Mount Rainier. An early Neoglacial advance (ca. 5000 cal yr BP) has not been identified on Mount Rainier, likely because moraines of that age were overrun by one or more subsequent ice advances. The Burroughs Mountain (middle Neoglacial) advance correlates approximately with other glacier advances in western North America (e.g., Calkin and Ellis, 1982; Calkin et al., 2001; Clague and Mathews, 1996; Davis, 1988; Osborn and Luckman, 1988). The wide range in limiting ages of the Older Garda ice advance (2200-1480 A.D.) means that this advance may be equivalent to an early LIA advance such as others reported in western North America (e.g., Calkin et al., 2001; Davis, 1988; Osborn and Luckman, 1988) or it could record an early medieval advance (Porter, 1986). The well-preserved late LIA, or Younger Garda, moraines on Mount Rainier are comparable to those of glacier advances in Europe (e.g., Denton and Karlén, 1973; Orombelli and Porter, 1982; Zumbühl, 1980), and western North America (e.g., Calkin and Ellis, 1982; Calkin et al., 2001; Clague and Mathews, 1996; Davis, 1988; Denton and Karlén, 1973; Evans, 1997; Luckman, 2000; Smith and Desloges, 2000).

This Neoglacial evidence suggests that the western U.S. and Canada are not disconnected by distance and global circulation patterns from short-term climate shifts, as Heine (1997) argued.

4.4 CONCLUSION

Rock samples were collected from boulders and bedrock surfaces associated with the outer moraines at each of four sites to obtain ^{36}Cl surface-exposure dates. Some of the resulting ages are anomalous, likely the result of thick snowcover that shielded the sites. The resulting data were used to assess the significance of this effect on surface-exposure ages. The anomalous ages from sampled boulders indicate the importance of sampling large (>1 m) boulders to minimize this shielding effect and to reduce potential uncertainty caused by problems associated with exhumation and displacement of the boulders. Most of the moraines had too few exposed boulders to address these uncertainties. A thick snowcover during mid- to late-Holocene time at the moraine sites reduced surface-exposure ages by ca. 50% of their expected values. Use of surface-exposure dating under conditions of thick, persistent snowcover can therefore lead to a large spread in ages that reduces the reliability of a moraine chronology based on cosmogenic isotopes alone.

During this project, Crandell's (1969) reconnaissance mapping was refined locally, the limits of each drift being determined more precisely. A latest Pleistocene or early Holocene glacier advance was followed by a middle Neoglacial advance that deposited Burroughs Mountain moraines, and by two late Neoglacial advances, marked by Older and Younger Garda moraines. These age assignments are based on tephrochronology, which provides a reliable but imprecise basis for dating individual moraines. The outermost moraine at each locality apparently records a McNeely or an early Holocene advance, but cannot be more-closely dated. Nevertheless, based on the ELA estimates for the late-glacial interval, these moraines cannot be McNeely-age moraines unless they

are very late-McNeely 2 recessional moraines. The moraine (or protalus rampart) mapped in Berkeley Park may be Younger Dryas in age based on its mean uncorrected ^{36}Cl age and the overlying tephra stratigraphy.

REFERENCES

- Andrews, J. T., and Giraudeau, J. (2003). Multi-proxy records showing significant Holocene environmental variability; the inner N. Iceland shelf, Hunafloi. *Quaternary Science Reviews* **22**, 2-4, 175-193.
- Alley, R. B., Mayewski, P. A., Sowers, T., Stuvier, M., Taylor, K. C., and Clark, P. U. (1997). Holocene climatic instability: A prominent, widespread event 8200 yr ago. *Geology* **25**, 483-486.
- Barber, D. C., Dyke, A., Hillaire-Marcel, C., Jennings, A. E., Andrews, J. T., Kerwin, M. W., Bilodeau, G., McNeely, R., Southon, J., Morehead, M. D., and Gagnon, J.-M. (1999). Forcing of the cold event of 8,200 years ago by catastrophic drainage of Laurentide lakes. *Nature* **400** 6742, 344-348.
- Barnosky, C. W. (1983). Late-Quaternary vegetational and climatic history of southwestern Washington. Unpublished PhD dissertation, University of Washington, 201 p.
- Begét, J. E. (1981). Early Holocene glacier advance in the North Cascade Range, Washington. *Geology* **9** 409-413.
- Bierman, P. R., Marsella, K. A., Patterson, C., Davis, P. T., and Caffee, M. (1999). Mid-Pleistocene cosmogenic minimum-age limits for pre-Wisconsinan glacial surfaces in southwestern Minnesota and southern Baffin Island: A multiple nuclide approach. *Geomorphology* **27**, 25-39.
- Bradley, R. S. and Jones, P. D. (1995). *Climate Since A. D. 1500*. Routledge, New York, 649-665.
- Brantley, S., Yamaguchi, D., Cameron, K., and Pringle, P. (1986). Tree-ring dating of volcanic deposits. *Earthquakes and Volcanoes* **5**, 184-194.
- Burbank, D. W. (1981). A chronology of Late Holocene glacier fluctuations on Mount Rainier, Washington. *Arctic and Alpine Research* **13**, 369-386.
- Calkin, P. E. and Ellis, J. M. (1982). Holocene glacial chronology of the Brooks Range, Northern Alaska. *Striae* **18**, 3-8.
- Calkin, P. E., Wiles, G. C., and Barclay, D. J. (2001). Holocene coastal glaciation of Alaska. *Quaternary Science Reviews* **20**, 449-461.

- Clague, J. J. and Mathews, R. W. (1996). Neoglaciation, glacier-dammed lakes, and vegetation change in northwestern British Columbia, Canada. *Arctic and Alpine Research* **28**, 10-24.
- Clark, D. H. and Gillespie, A. R. (1997). Timing and significance of late-glacial and Holocene cirque glaciation in the Sierra Nevada, California. *Quaternary International* **38/39**, 21-38.
- Crandell, D. R. (1969). Surficial geology of Mount Rainier National Park, Washington. U. S. Geological Survey Bulletin **1288**, 41p.
- Crandell, D. R. (1971). Postglacial lahars from Mount Rainier Volcano, Washington. U. S. Geological Survey Professional Paper **677**, 75p.
- Crandell, D. R. and Miller, R. D. (1964). Post-hypsithermal glacier advances at Mount Rainer, Washington. *In Geological Survey research 1964: U.S. Geological Survey Professional Paper* **501-D**, D110-D114.
- Davis, P. T. (1988). Holocene glacier fluctuations in the American Cordillera. *Quaternary Science Reviews* **7**, 129-157.
- Denton, G. H. and Karlén, W. (1973). Holocene climate variations-their pattern and possible cause. *Quaternary Research* **3**, 155-205.
- Driedger, C. L. (1986). A visitor's guide to Mount Rainier glaciers. Pacific Northwest National Parks and Forests Association, Longmire, WA, 80 p.
- Driedger, C. L. and Kennard, P. M. (1984). Ice volumes on Cascade volcanoes: Mount Rainier, Mount Hood, Three Sisters and Mount Shasta. U. S. Geological Survey Open-File Report 84-581, 55 p.
- Dunwiddie, P.W. (1986). A 6000-year record of forest history on Mount Rainier, Washington. *Ecology* **67**, 58-68.
- Ebbesmeyer, C.C. and R.M. Strickland. 1995. Oyster Condition and Climate: Evidence from Willapa Bay. Publication WSG-MR 95-02, Washington Sea Grant Program, University of Washington, Seattle, WA, 11 p.
- Evans, M. (1997). Pollen evidence of late Holocene treeline fluctuation from the southern Coast Mountains, British Columbia. *Géographie physique et Quaternaire* **51**, 81-92.

- Frederick, J. E. (1980). Perennial snowcover variations during the last 130 years at Mt. Rainier, Washington. Unpublished M.S. thesis, University of Washington, 67 p.
- Gosse, J. C., Evenson, E. B., Klein, J., Lawn, B., and Middleton, R. (1995). Precise cosmogenic ^{10}Be measurements in western North America: Support for a global Younger Dryas cooling event. *Geology* **23**, 10, 877-880.
- Gosse, J.C. and Phillips, F.M., 2001. Terrestrial in situ cosmogenic nuclides: theory and application. *Quaternary Science Reviews* **20**, 1475-1560.
- Hallet, B. and Putkonen, J. (1994). Surface dating of dynamic landforms: Young boulders on aging moraines. *Science* **268**, 937-940.
- Heine, J. T. (1997). Glacier advances at the Pleistocene/Holocene transition near Mount Rainier volcano, Cascade Range, USA. Unpublished PhD dissertation. University of Washington, 137 p.
- Heine, J. T. (1998). Extent, timing, and climatic implications of glacier advances Mount Rainier, Washington, U.S.A., at the Pleistocene/Holocene transition. *Quaternary Science Reviews* **17**, 1139-1148.
- Hughen, K. A., Overpeck, J. T., Peterson, L. C., and Trumbore, S. (1996). Rapid climate changes in the tropical Atlantic region during the last deglaciation. *Nature* **380**, 51-54.
- Johannesson, T., Raymond, C. F., and Waddington, E. D. (1989). A simple method for determining the response time of glaciers. *In: Glacier fluctuations and climate change*. Oerlemans, J. (editor). Kluwer Academic, Dordrecht, Netherlands, 343-352.
- Karlén, W., and Denton, G. H. (1976). Holocene glacial variations in Sarek National Park, northern Sweden. *Boreas* **5**, 25-56.
- Lawrence, D. B. (1950). Estimating dates of recent glacier advances and recession rates by studying tree-growth rings. *Transactions, American Geophysical Union* **31**, 243-248.
- Lehman, S. J., and Keigwin, L. D. (1992). Sudden changes in North Atlantic circulation during the last deglaciation. *Nature* **356**, 757-762.
- Luckman, B. H. (2000). The Little Ice Age in the Canadian Rockies. *Geomorphology* **32**, 357-384.

- Liu, B., Phillips, F. M., Fabryka-Martin, J. T., Fowler, M. M., Biddle, R. S., and Stone, W. D. (1994). Cosmogenic ^{36}Cl accumulation in unstable landforms, I. Effects of thermal neutron distribution. *Water Resources Research* **30**, 1071-1074.
- Mathes, F. E. (1939). Report of the Committee on Glaciers. *Transactions, American Geophysical Union* **20**, 518-523.
- McCarthy, D. P. and Luckman, B. H. (1993). Estimating ecessis for tree-ring dating of moraines; a comparative study from the Canadian Cordillera. *Arctic and Alpine Research* **25**, 63-68.
- Miller, C. D. (1969). Chronology of Neoglacial moraines in the Dome Peak area, north Cascade Range, Washington. *Arctic and Alpine Research* **1**, 49-65.
- Miller, M. M. (1964). Inventory of terminal position changes in Alaskan coastal glaciers since the 1750's. *Proceedings from the American Philisophical Society* **108**, 257-273.
- Mount Rainier National Park website:
<http://www.nps.gov/mora/current/weather.htm#cause>
- Mullineaux, D. R. (1974). Pumice and other pyroclastic deposits in the Mount Rainier National Park, Washington. *U.S. Geological Survey Bulletin* **1326**, 83 p.
- Nylen, T. H. (1998). Spatial and temporal variations of glaciers on Mount Rainier between 1913 and 1994. Unpublished M.S. thesis. Portland State University, 101 p.
- Orombelli, G. and Porter, S. C. (1982). Late Holocene fluctuations of Brenva Glacier. *Geografia Fisica e Dinamica Quaternaria* **5**, 14-37.
- Osborn, G., and Luckman, B. H. (1988). Holocene glacier fluctuations in the Canadian Cordillera (Alberta and British Columbia). *Quaternary Science Reviews* **7**, 115-128.
- Porter, S. C. (1975). Equilibrium line altitudes of late Quaternary glaciers in the Southern Alps, New Zealand. *Quaternary Research* **5**, 27-47.
- Porter, S. C. (1981a). Lichenometric studies in the Cascade Range of Washington: Establishment of *Rhizocarpon geographicum* growth curves at Mount Rainier. *Arctic and Alpine Research* **13**, 1, 11-23.
- Porter, S. C. (1981b). Recent glacier variations and volcanic activity. *Nature* **291** 139-142.

- Porter, S. C. (1986). Pattern and forcing of northern hemisphere glacier variations during the last millennium. *Quaternary Research* **26**, 27-48.
- Porter, S. C. (2000). Onset of Neoglaciation in the Southern Hemisphere. *Journal of Quaternary Science* **15**, 4, 395-408.
- Porter, S. C. (2001). Snowline depression in the tropics during the last glaciation. *Quaternary Science Reviews* **20**, 1067-1091.
- Porter, S. C., and Denton, G. H. (1967). Chronology of Neoglaciation in the North American Cordillera. *American Journal of Science* **265**, 177-210.
- Porter, S. C., Pierce, K. L., and Hamilton, T. D. (1983). Late Pleistocene mountain glaciation in the western United States. *In*: "Late Quaternary environments of the United States. Volume 1, the late Pleistocene" (S. C. Porter, ed.). Minneapolis, University of Minnesota Press, 71-111.
- Porter, S. C. and Swanson, T. W. (1998). Radiocarbon age constraints on rates of advance and retreat of the Puget Lobe of the Cordilleran ice sheet during the last glaciation. *Quaternary Research* **50**, 205-213.
- Putkonen, J. (2003). Cosmogenic exposure dated boulders reveal moraine erosion history, Bishop Creek, Ca, USA. Geological Society of America Annual Meeting, Seattle, Abstracts with Programs, **35**, 109.
- Reasoner, M.A., Davis, P.T., and Osborn, G. (2001). Evaluation of proposed early Holocene advances of alpine glaciers in the North Cascade Range, Washington State, USA: constraints provided by paleoenvironmental reconstructions. *The Holocene* **11**, 607-611.
- Sigafoos, R. S. and Hendricks, E. L. (1961). Botanical evidence of the modern history of Nisqually Glacier, Washington. U.S. Geological Survey Professional Paper **387-A**, 20p.
- Sigafoos, R. S. and Hendricks, E. L. (1969). The time interval between stabilization of alpine glacial deposits and establishment of tree seedlings. U. S. Geological Survey Professional Paper **650-B**, B89-B93.
- Sigafoos, R. S. and Hendricks, E. L. (1972). Recent activity of glaciers on Mount Rainier, Washington. U. S. Geological Survey Professional Paper **387-B**, 24 p.
- Sisson, T. W., U. S. Geological Survey. Personal communication, unpublished data (2003).

- Smith, D. J. and Desloges, J. R. (2000). Little Ice Age history of Tzeetsaytsul Glacier, Tweedsmuir Provincial Park, British Columbia. *Géographie physique et Quaternaire* **54**, 135-141.
- Stuiver, M., Reimer, P. J., Bard, E., Beck, J. W., Burr, G. S., Hughen, K. A., Kromer, B., McCormac, F. G., v. d. Plicht, J., and Spurk, M. (1998). INTCAL98 Radiocarbon age calibration 24,000—0 cal BP. *Radiocarbon* **40**, 1041–1083.
- Swanson, T.W. (1994). Determination of chlorine-36 production rates from the deglaciation history of Whidbey Island, Washington. Unpublished PhD dissertation. University of Washington, 121 p.
- Swanson, T. W. and Caffee, M. L. (2001). Determination of ^{36}Cl production rates derived from the well-dated deglaciation surfaces of Whidbey and Fidalgo Islands, Washington. *Quaternary Research* **56**, 366-382.
- Thomas, P.A., Easterbrook, D.J., and Clark, P.U. (2000). Early Holocene glaciation on Mount Baker, Washington state, USA. *Quaternary Science Reviews* **19**, 1043-1046.
- Vallance, J. W. and Scott, K. M. (1997). The Osceola Lahar from Mount Rainier: Sedimentology and hazard implications of a huge clay-rich debris flow. *Geological Society of America Bulletin* **109**, 143-163.
- von Grafenstein, U., Erlenkeuser, H., Mueller, J., Jouzel, J., and Johnsen, S. (1998). The cold event 8200 years ago documented in oxygen isotope records of precipitation in Europe and Greenland. *Climate Dynamics* **14**, 73-81.
- Waitt, R. B. Jr., Yount, J. C., and Davis, P. T. (1982). Regional significance of an early Holocene moraine in Enchantment Lakes Basin, North Cascade Range, Washington. *Quaternary Research* **17**, 191-210.
- Zreda, M.G., Phillips, F.M., Elmore, D., Kubik, P.W., and Sharma, P. (1991). Cosmogenic chlorine-36 production rates in terrestrial rocks. *Earth and Planetary Science Letters* **105**, 94-109.
- Zumbühl, H. J. (1980). Die Schwankungen der Grindelwaldgletscher in den historischen Bild- und Schriftquellen des 12. bis 19. Jahrhunderts (Translated title: The fluctuations of the Grindelwald Glacier in historical pictures and writings from the 12th-19th centuries: a contribution for glacier history and the study of the Alpine region). Birkhäuser Verlag, Basel, Switzerland, 92 p.